

**AP-2 β NEURAL CREST CELL KNOCKOUT AND
SUBSEQUENT LOSS OF RETINAL GANGLION CELLS**

PROGRESSION OF RETINAL GANGLION CELL LOSS
OBSERVED AS A RESULT OF ANTERIOR SEGMENT
DYSGENESIS FOLLOWING CONDITIONAL DELETION OF
ACTIVATING PROTEIN-2 β IN CRANIAL NEURAL CREST
CELLS

By
ANTHONY SARACO. B.ENG., BIOSCI.

A Thesis
Submitted to the School of Graduate Studies
In Partial Fulfillment of the Requirements
For the Degree
Master of Science

McMaster University
©Copyright by Anthony Saraco, May 2019

MASTER OF SCIENCE (2019)

(Medical Sciences)

TITLE: Progression of retinal ganglion cell loss observed as a result of anterior segment dysgenesis following conditional deletion of activating protein-2 β in cranial neural crest cells

AUTHOR: Anthony Saraco, B.Eng., Biosci. (McMaster University)

SUPERVISOR: Dr. Judith A. West-Mays

NUMBER OF PAGES: x, 71

Abstract

Our lab has shown that conditionally disrupting the *tcfa2 β* gene, responsible for the activating protein-2 β (AP-2 β) transcription factor, exclusively in the craniofacial neural crest cells, leads to anterior segment dysgenesis. Subsequent loss of the corneal endothelium results in the adherence of the iris to the corneal stroma, causing closure of the iridocorneal angle. The activating protein-2 β neural crest cell knockout (AP-2 β NCC KO) model involves a complete blockage of the both the conventional (through the trabecular meshwork) and non-conventional (uveoscleral) pathways for aqueous humor drainage and therefore it could be used as a powerful experimental model for glaucoma. As shown by our previous work, elevated intraocular pressure (IOP) and a 35% decrease in the number of cells in the retinal ganglion cell (RGC) layer was observed in AP-2 β NCC KO mice by 2 months; 6 to 11 months sooner than other reported mouse models of glaucoma. These observations suggested that the AP-2 β NCC KO mouse could be a novel and cost-effective experimental model for glaucoma if the RGC loss occurred progressively rather than due to a congenital defect.

The purpose of this research project was to investigate how the retinal ganglion cell layer and macroglial activity changes with respect to age in the AP-2 β NCC KO mutant through immunofluorescence. Specifically, it was investigated whether the loss of RGCs was progressive and due to the increased IOP caused by the blockage of the uveoscleral drainage pathway.

A significant decrease in the number of RGCs was observed between P4 and P10 in the retinal periphery of both WT and AP-2 β NCC KO mice ($p < 0.05$), which is indicative of the programmed cell death that occurs due to retinal pruning during development. No statistical difference between WT and AP-2 β NCC KO mice phenotypes was observed at postnatal day 4 (P4), suggesting that no developmental defect resulted in the significant loss of RGCs at 2 months. In all other time points investigated, while no statistical difference was found between WT and the AP-2 β NCC KO mutant, a clear downwards trend was present in the AP-2 β NCC KO mutant retinal ganglion cell layer from P10 to P40. There was also expression of glial fibrillary acidic protein (GFAP) by Müller cells, indicating the presence of neuroinflammation at P35 and P40. This substantiates the potential P42 starting point of neurodegeneration our lab previously observed. This was further corroborated with Müller cell-associated expression of GFAP at P35 and P40 exclusively in the AP-2 β NCC KO mouse.

Overall, we have shown that the retinal damage observed in our AP-2 β NCC KO mouse is not due to a developmental defect, but rather occurs over time. Thus, this mouse model, which appears to block both the conventional and unconventional uveoscleral pathways, has a profound effect on aqueous humor drainage. As a result, the model requires relatively little time to observe an increase in IOP and subsequent RGC loss. Our findings suggest that the AP-2 β NCC KO mouse can be a novel, powerful, and extremely cost-effective experimental model for glaucoma.

Acknowledgements

To Dr. West-Mays, my supervisor: I hope I can convey how grateful I am for everything that you have given me during my tenure as a graduate student. You saved me when I was stranded with no plans just before graduation and I cannot imagine what I would be doing if you had not come in at the eleventh hour. Your support has been unrivaled not only in research but in my passion for teaching anatomy and my aspirations to pursue medicine. I cannot thank you enough for the immense amount of patience you have shown me over these past years. I owe much of who I have grown to be as an academic, a communicator, and as a leader to you through your mentorship and inspiration. Two more things: karaoke with you was a blast, and I still owe you a drink.

To my committee members, Dr. Mishra and Dr. Ball: I want to thank you for every **much-needed** ounce of help throughout the project. Dr. Mishra, you have always pushed me to broaden my frame of thinking; from working through how Parkinson's disease progresses to critical analysis of drug release devices. Dr. Ball, our friendship has grown since my second year of my undergrad. You have taught me everything I know about anatomy and your passion for teaching as ignited a fire in me that I will fight tooth and nail to ensure is always kindled. Thank you for teaching me the dangers of Hoover Dustette vacuums.

To Paula Deschamps: I would not have been able to complete any work without you. You are an invaluable resource to the lab, and it would crumble like Babylon without you. I cannot count how many times our furry friends would be causing issues but no matter what, you could talk some sense into them immediately. You have not only helped me but everyone that has and will pass through the lab. Please always remember that we students would be completely lost without you, and you have our eternal gratitude. To my lab mates, past and present: thank you for welcoming me into the lab, teaching and supporting me through my research, dealing with every stupid, remedial biology question I could think of, and helping me prepare for my committee meetings. They were still tragic, but you tried your best and I am incredibly appreciative. I wish each of you the best in your undoubtedly successful futures. Trivia lunches are long since passed, but the useless knowledge I gained from them is stuck in my brain forever.

I would also like to thank my family, especially my mom, for all their support. I could not have achieved this without you. I love you, mom - even when we disagree about how much school is *too much*, I know that you will always support me and make me think about the hard questions. To Lily, thank you for translating my gibberish and rabbling thoughts into English and coherent sentences. That could not have been easy, but *c'est la vie*.

Finally, thank you, Thomas Dakin, Alexander Gordon, and Lesley Gracie for giving me the courage to power through this thesis.

Table of Contents

AP-2B NEURAL CREST CELL KNOCKOUT AND SUBSEQUENT LOSS OF RETINAL GANGLION CELLS	I
ABSTRACT	IV
ACKNOWLEDGEMENTS	VI
LIST OF TABLES AND FIGURES	IX
LIST OF ABBREVIATIONS	X
INTRODUCTION	1
ANATOMY OF EYE AND RETINA	2
GLAUCOMA	4
RETINAL GANGLION CELLS	5
MÜLLER CELLS	6
CURRENT EXPERIMENTAL MODELS FOR GLAUCOMA	8
AQUEOUS HUMOUR PRODUCTION AND DRAINAGE	9
ACTIVATING PROTEIN-2B TRANSCRIPTION FACTOR AND NEURAL CREST CELL KNOCKOUT MODEL	10
HYPOTHESIS AND RESEARCH AIMS	13
RATIONALE	14
MAIN HYPOTHESIS	15
RESEARCH AIMS	15
AIM 1: TO ANALYZE AND QUANTIFY THE NUMBER OF CELLS IN THE RGC LAYER AT KEY POSTNATAL DAYS DURING RETINAL DEVELOPMENT.	15
AIM 2: TO EXAMINE MACROGLIAL ACTIVITY IN AP-2B NCC KO MICE DURING RETINAL DEVELOPMENT.	16
METHODS	17
ANIMAL HUSBANDRY	18
EXTRACTION AND PROCESSING OF TISSUE	18
EYES	18
EARS/TAILS	18
PCR AND GEL ELECTROPHORESIS	19
HISTOLOGY	19
EMBEDDING AND SECTIONING	19
IMMUNOHISTOCHEMISTRY	19
DATA ACQUISITION AND STATISTICAL ANALYSIS	20
RESULTS	22
QUANTIFICATION OF RETINAL GANGLION CELLS AT EARLY POSTNATAL STAGES	23
EXPRESSION OF GLIAL FIBRILLARY ACIDIC PROTEIN (GFAP) BY MÜLLER CELLS	28
MÜLLER CELL EXPRESSION OF VIMENTIN IN AP-2B NCC KO MOUSE	30
DISCUSSION	32

PROGRESSIVE LOSS OF RETINAL GANGLION CELLS IN THE AP-2B NCC KO MOUSE	33
GFAP EXPRESSION BY MÜLLER CELLS MARKS NEUROINFLAMMATION AT P35 TO P40	36
VIMENTIN EXPRESSION CONFIRMS THE PRESENCE OF MÜLLER CELLS IN AP-2B NCC KO MOUSE	38
CONCLUSIONS AND FUTURE DIRECTIONS	40
REFERENCES	45
FIGURES	51

List of Tables and Figures

Figure 1	General Anatomy of the Mammalian Eye	52
Figure 2	Vertebrate eye development and tissue derivations	53
Figure 3	Retinal development	54
Figure 4	Schematic showing the theory of the relationship between increased intraocular pressure and glaucoma	55
Figure 5	Anterior Chamber and Aqueous Humor Pathways	56
Figure 6	The expression of AP-2 β in an E15.5 murine eye	57
Figure 7	PCR results denoting mouse genotype	58
Figure 8	Brn3a expression in postnatal day 4 wild-type and AP-2 β NCC KO	59
Figure 9	Brn3a expression in postnatal day 10 wild-type and AP-2 β NCC KO	60
Figure 10	Brn3a expression in postnatal day 35 wild-type and AP-2 β NCC KO	61
Figure 11	Brn3a expression in postnatal day 40 wild-type and AP-2 β NCC KO	62
Figure 12	The change in number of brn3a labelled cells with respect to time in the wild-type and AP-2 β NCC KO	63
Figure 13	GFAP expression in postnatal day 4 wild-type and AP-2 β NCC KO	64
Figure 14	GFAP expression in postnatal day 10 wild-type and AP-2 β NCC KO	65
Figure 15	GFAP expression in postnatal day 35 wild-type and AP-2 β NCC KO	66
Figure 16	GFAP expression in postnatal day 40 wild-type and AP-2 β NCC KO	67
Figure 17	Vimentin expression in postnatal day 40 wild-type and AP-2 β NCC KO	68
Figure 18	Colocalization of vimentin and GFAP expression in the postnatal day 40 wild-type and AP-2 β NCC KO	69
Table 1	1X Master mix recipes	70
Table 2	PCR protocol	70
Table 3	Antibodies used for immunohistochemistry	71
Table 4	Summary of ANOVA results for region adjacent to Optic nerve head (ONH)	71
Table 5	Summary of ANOVA results for region at middle of retina (mid-periphery)	71
Table 6	Summary of ANOVA results for region adjacent to the ciliary body (periphery)	71

List of Abbreviations

AP-2	Activating Protein-2
ASD	Anterior segment dysgenesis
BDNF	Brain-derived neurotrophic factor
CI	Confidence interval
E	Embryonic day
ER	Endoplasmic reticulum
GCL	Ganglion cell layer
GFAP	Glial fibrillary acidic protein
INL	Inner nuclear layer
IOP	Intraocular pressure
IPL	Inner plexiform layer
KO	Knockout
NCC	Neural crest cells
NFL	Nerve fibre layer
ON	Optic nerve
onbl	Outer neuroblastic layer
ONH	Optic nerve head
OPL	Outer plexiform layer
P	Postnatal day
PCR	Polymerase chain reaction
POM	Periocular mesenchyme
RGC	Retinal ganglion cell
RPE	Retinal pigmented epithelium
SD	Standard deviation
WT	Wild-type

Introduction

Anatomy of eye and retina

The eye is a specialized organ responsible for converting photons into electrical signals that give rise to the special sense of vision. The eye is comprised of two regions: the anterior segment that includes the cornea, iris, ciliary body, and the lens while the posterior segment includes the choroid, neural retina, and optic nerve (Figure 1). The primary function of the anterior segment is to focus the light and control the amount of light that will stimulate the retina, while the primary function of the posterior segment is the initial processing of the light signal. Oculogenesis is orchestrated via the development of the forebrain, neuroepithelium, periocular mesenchyme (POM), and surface ectoderm (Chow & Lang, 2001; Cvekl & Tamm, 2004). During gastrulation, the meeting of the neuroepithelium and surface ectoderm mark the beginning of the induction of the optic field (Chow & Lang, 2001). Lateral migration of the optic field continues until two distinct structures are formed that will further develop into the eye: the eye primordia. Migration and outpouching of the neuroepithelium form the optic vesicles that will start to invaginate alongside the surface ectoderm upon contact of the two layers (Martínez-Morales, Rodrigo, & Bovolenta, 2004). The invagination of the optic vesicles forms a bilayer tissue known as the optic cup. The invaginating layer of the optic cup (the superficial layer) will develop into the neural retina while the surrounding layer (the deep layer) will form the retinal pigmented epithelium and the optic stalk (Bharti, Nguyen, Skuntz, Bertuzzi, & Arnheiter, 2006). The invaginating surface ectoderm thickens and is referred to as the lens placode. The pinching off of the lens placode from the surface ectoderm forms the lens vesicle that later forms the mature lens while the remaining, overlying surface ectoderm forms the corneal

epithelium (Chow & Lang, 2001) (Figure 2). The corneal stroma and endothelium are derived from the periocular mesenchyme (POM), a population of cells that consist of cranial neural crest cells (NCC) and mesoderm. The POM also gives rise to the iris stroma, ciliary body muscle and stroma, as well as the trabecular meshwork (Gage, Rhoades, Prucka, & Hjalt, 2005; Gould, Smith, & John, 2004).

The neural retina is an extension of the forebrain ectoderm and is derived from the superficial portion of the optic cup, while the retinal pigmented epithelium (RPE) is derived from the deep portion of the optic cup. The purpose of the RPE is multifaceted and includes ion homeostasis between the neural retina and choroid, absorption of off-axis light, and maintenance of the blood-retinal-barrier (BRB) (Bok, 1993). Neural retinogenesis begins at embryonic day 10.5 (E10.5) and continues until postnatal day 11 and includes the differentiation of retinal progenitor cells (RPC) into macroglia, Müller cells and astrocytes, as well as the neurons within the retina: rod and cone photoreceptors, horizontal cells, amacrine cells, bipolar cells, and retinal ganglion cells. The RPCs differentiate into the various cell types in a fixed and overlapping order: retinal ganglion cells, horizontal cells, cone photoreceptors, amacrine cells, rod photoreceptors, bipolar cells, and finally Müller cells (Marquardt, 2003; Zhang, Serb, & Greenlee, 2011). The neural retina is comprised of multiple layers: three nuclear layers: retinal ganglion cell (RGC) layer, the inner nuclear (IN) layer and outer nuclear (ON) layer; and two synaptic layers: inner and outer plexiform layers (IP and OP respectively). Rod and cone photoreceptor cell bodies reside in the ONL; horizontal, amacrine, bipolar, and Müller cell bodies reside in the INL; and retinal ganglion cell bodies reside in the RGC layer (Figure 3a). Photons cause conformational changes to

opsins and result in a transmembrane potential change of cones (responsible for high acuity colour vision); the same process occurs with rhodopsin for rods (responsible for low-light vision). Rods and cones synapse in the outer plexiform layer with horizontal cells, amacrine cells, and bipolar cells to perform initial processing of the visual signal. These cells synapse in the inner plexiform layer with the retinal ganglion cells (RGC) and follows one of four pathways: the central visual pathway to the lateral genicular nucleus (conscious vision) (Hickey & Spear, 1976), tectal pathway to the superior colliculus (visual reflexes) (Hayhow, Sefton, & Webb, 1962), retinohypothalamic pathway to the hypothalamus (circadian rhythm) (Mason, Sparrow, & Lincoln, 1977), and the pretectal pathway to the Edinger-Westphal nucleus (light adaptation) (Hayhow et al., 1962).

Glaucoma

Glaucoma is a neurodegenerative disease that causes the death of retinal ganglion cells (RGCs) and is the leading cause of irreversible blindness worldwide. The loss of RGCs results in characteristic visual field deficits until the untreated patient succumbs to complete blindness. Due to the nature of the disease, current treatment is limited to slowing the progression and prevention rather than reversal of damage. By 2040, over 112 million people are predicted to experience loss of vision as a result of glaucoma, the majority of populations affected being from Asia and Africa (Quigley & Broman, 2006; Tham et al., 2014). While risk factors include, genetics, race, and age, the risk factor that is targeted for intervention is intraocular pressure (IOP) (Boland & Quigley, 2007; Chang & Goldberg, 2012; Coleman & Miglior, 2008; M, 2015). While it is possible that patients with increased intraocular pressure may not develop glaucoma (Araie,

Sekine, Suzuki, & Koseki, 1994), most experimental models for glaucoma use increased IOP as a means of eliciting RGC death (Figure 4).

Glaucoma has a few variations described by key characteristics: the degree of the iridocorneal angle (open or closed) and the pressure within the eye (hypertension or normotensive). Glaucoma can also be categorized as developmental glaucoma, caused by a congenital deficiency. While congenital glaucoma can include a malformation of the trabecular meshwork (Mandal & Chakrabarti, 2011), closure of the iridocorneal angle is a common feature in developmental glaucoma that is related to anterior segment dysgenesis (ASD). While many genes are associated with ASD, nine genes: PAX6, PITX2, PITX3, FOXC1, FOXE3, EYA1, CYP1B1, LMX1B, and MAF, have been associated with ASD that involves glaucoma (Gould & John, 2002).

Retinal Ganglion Cells

Retinal ganglion cells (RGCs) are responsible for transmitting the initially processed visual information from the retina to other aspects of the central nervous system. These structures in the central nervous system include the lateral geniculate nucleus and visual cortex for conscious perception (Hickey & Spear, 1976), the superior colliculus for visual reflexes (Hayhow et al., 1962), the hypothalamus for circadian rhythms (Mason et al., 1977), and the Edinger-Westphal nucleus for light adaptation (Hayhow et al., 1962). In the human retina, the RGCs are located in the RGC layer, the most superficial layer of the human retina. RGCs can be classified into large-field alpha and small-field beta subclasses and then further divided based on their response to light. Some RGCs depolarize when stimulated by bipolar cells in the inner substrata of the inner plexiform layer (ON RGCs), and RGCs that hyperpolarize when stimulated by

bipolar cells in the outer substrata of the inner plexiform layer (OFF RGCs). Within the retina, the transcription factor family that is exclusively expressed by RGCs is the *brn3* family of transcription factors (*brn3a*, *b*, and *c*) (Xiang et al., 1995). It has been shown that these transcription factors are important for specific subpopulations of RGCs through the selective deletion of each one. For example, loss of function of *brn3a* results in a disruption in the RGC dendrite morphology while the deletion of *brn3b* resulted in a 70-80% decrease in the number of RGCs (Erkman et al., 1996). While the deletion of *brn3c* did not result in loss of RGCs, the *brn3b-brn3c* double KO mutant showed a more severe loss of RGCs than the single *brn3b* KO (Badea, Cahill, Ecker, Hattar, & Nathans, 2009; Wang et al., 2002). Since the deletion of *brn3a* has a more dramatic impact on retinogenesis, *brn3a* is more appropriate to use for labelling RGCs than the other two factors in the *brn3* transcription factor family.

The development of the mouse RGCs starts at E11 and continues until postnatal day 21 (P21) (Young, 1984). The major events in RGC development include generation of the RGC precursors (E11 – E19) as well as the subsequent programmed cell death and maturation until P21. The programmed cell death of RGCs increases in activity through P0 to P4, peaking on days P2 to P5, then continues until near completion at P21.

Müller Cells

Müller cells are macroglial cells that radially span the entire retina and have many functions normally associated with other glial cells. While glial cells have their embryonic origin from the neural tube, it has been suggested that a subset of Müller cells are derived from cranial NCC (Liu et al., 2013). Müller cells are responsible for homeostatic regulation of the extracellular fluid, assist astrocytes in the integrity of the

blood-retinal barrier (BRB), and have the ability to regulate the amount of potassium, glutamate, and GABA present in synapses (Bringmann, Grosche, Pannicke, & Reichenbach, 2013; Bringmann et al., 2013; Chong & Martin, 2015). Müller cells have also been shown to act as scaffold for mechanical protection of neurons and reduce light scattering on the way to the photoreceptors by guiding the light (Franze et al., 2007). The soma of the Müller cell is present in the inner nuclear layer and with projections travelling towards the nerve fiber layer and towards the end of the photoreceptor layer. Müller cells express vimentin, a type III intermediate filament (IF), that has a role in supporting the structure of the retina especially during times of mechanical stress, similar to IFs in epithelial cells and myocytes (Lundkvist et al., 2004). Another type III IF, glial fibrillary acidic protein (GFAP), is expressed by astrocytes but also upregulated in Müller cells during retinal degeneration. Therefore, GFAP expression by Müller cells is indicative of retinal inflammation and neurodegeneration (P. J. Anderson et al., 2008; Luna, Lewis, Banna, Skalli, & Fisher, 2010). The overexpression of GFAP by Müller cells, known as Müller cell gliosis, is purported to increase the structural support around RGCs and further protect them from mechanical stress. However, it has been shown that chronic gliosis can exacerbate retinal degeneration (Bringmann et al., 2006; Coorey, Shen, Chung, Zhu, & Gillies, 2012). In the case of hypertensive glaucoma where fluctuating and constant mechanical stress is placed on the retina, this phenomenon could be contributing to the loss of cells within the RGC layer (Bringmann et al., 2006; Coorey et al., 2012).

Current Experimental Models for Glaucoma

Models that investigate the death of RGCs, as it occurs in glaucoma, include ischemia models, excitotoxic models, and optic nerve injury models. While these models can be effective in learning how RGCs behave post-injury, these models fail to include the progressive nature of glaucoma. Due to glaucoma being a progressive neurodegenerative disease associated with the elderly, animal models intending to recreate a similar progression require a significant amount of time and resources. To accomplish RGC loss as a result of high IOP, the general manipulation that these models use is blocking the conventional aqueous humor (AH) drainage pathway. Models that use a genetic means of AH draining blocking include the DBA/2J mouse model (M. G. Anderson et al., 2002), the Col α 11 $_{r/r}$ mouse model (Aihara, Lindsey, & Weinreb, 2003b) and the Tyr437His transgenic model (Senatorov et al., 2006). The DBA/2J model for glaucoma uses gene manipulation to create atrophy of the iris stroma (John et al., 1998). The dispersion of the iris stroma by 6-8 months causes occlusion of AH drainage structures and results in increased IOP after 8-13 months (John et al., 1998). Due to the variability in the iris stroma deposition, the DBA/2J model can result in varying degrees of IOP increases and RGC death (Libby et al., 2005). A similar *modus operandi* is used by the Col α 11 $_{r/r}$ and Tyr437His transgenic mice. The Col α 11 $_{r/r}$ mice have a mutation of the α 1 subunit of the type I collagen that causes deposition of type I collagen to block AH drainage similar to the DBA/2J model (Aihara et al., 2003b). While the Tyr437His transgenic model manipulates the secretion of mutated myocilin in the trabecular meshwork to generate a similar phenotype (Senatorov et al., 2006). The Col α 11 $_{r/r}$ and Tyr437His transgenic mice require over 18 months to produce RGC loss

due to increased IOP. Furthermore, all three of these models exclusively block the conventional aqueous humor pathway and do not include a means of blocking the uveoscleral outflow pathway. The large amount of time required for the DBA/2J, Col α 11^{r/r}, and Tyr437His transgenic mouse models to reach clinically relevant increases in IOP is likely due to these models of glaucoma exclusively blocking the conventional aqueous humor pathway as it only contributes to 20% of aqueous humor drainage (Aihara, Lindsey, & Weinreb, 2003a; Fautsch & Johnson, 2006).

Aqueous Humour Production and Drainage

Aqueous humor is a clear fluid that fills the anterior and posterior chambers of the eye and has a similar function to blood for avascular tissues such as the lens and cornea. Aqueous humor is responsible for providing nutrients, removing metabolic by-products, as well as allowing inflammatory cells and drugs to move around the eye (Goel, Picciani, Lee, & Bhattacharya, 2010). Aqueous humor is secreted by the ciliary epithelium that lines the processes of the ciliary body and initially enters the posterior chamber. The aqueous humor travels around the lens and enters into the anterior chamber through the pupil. Once in the anterior chamber, the aqueous humor may passively exit the anterior chamber back into circulation via two pathways: the conventional and non-conventional routes. In times of insufficient aqueous humor drainage, the IOP increases within the anterior chamber. This pressure causes the vitreous humor to compress the axons of the RGCs as they exit through lamina cribrosa and cause metabolic and endoplasmic reticulum (ER) stress. The compressed axons decrease the retrograde transport of brain-derived neurotrophic factor (BDNF), signalling the RGCs to induce apoptosis (Quigley et al., 2000) (Figure 4).

The conventional outflow route consists of aqueous humor passing through the trabecular meshwork into the lumen of Schlemm's canal, collecting into collector channels and finally draining into aqueous and episcleral veins (Ascher, 1954; Goldmann, 1950). The outflow rate through the conventional pathway is dictated by the pressure gradient and the endothelial lining of Schlemm's canal (Bill & Svedbergh, 1972). While the pressure gradient gives rise to the driving force through the conventional pathway, the endothelial lining of Schlemm's canal modifies the rate of outflow via structural changes (Grierson & Lee, 1978; Johnstone & Grant, 1973).

The non-conventional outflow route (also known as the uveoscleral pathway) consists of aqueous humor passing through the uveal meshwork, traveling through the connective tissue between the muscle bundles of the ciliary muscle, and finally exiting through the suprachoroidal space and sclera (Bill & Hellsing, 1965). In mice, 80% of aqueous humor drainage occurs through the uveoscleral pathway (Aihara et al., 2003a; Fautsch & Johnson, 2006). Interestingly, the outflow rate through the non-conventional route is independent of intraocular pressure as opposed to the conventional pathway (Brubaker, 2001) (Figure 5).

Activating Protein-2 β Transcription Factor and Neural Crest Cell Knockout Model

Activating Protein-2 (AP-2) is a family of transcription factors that are crucial for the development of many tissues and organs, including the eye. There are five AP-2 transcription factors in mice and humans: AP-2 α , AP-2 β , AP-2 δ , AP-2 γ , AP-2 ϵ ; all encoded by the *tcfap2 α - ϵ* genes respectively (*TCFAP2 α - ϵ* in humans). In humans, the autosomal dominant mutation affecting the AP-2 β transcription factor causes Char syndrome, for which it has been reported that patients exhibit patent ductus arteriosus,

facial dysmorphism, and abnormalities associated with the fifth digit (Satoda et al., 2000). However, the ocular features in these patients have not been examined. The structures affected in Char syndrome suggest that AP-2 β is crucial in the development of structures derived from the neural crest (Satoda et al., 2000). In the developing eye, both *tcfap2 β* and *tcfap2 α* have been shown to be expressed in the neural crest derived-periocular mesenchyme (POM). At embryonic day 8 (E8) both *tcfap2 β* and *tcfap2 α* showed overlapping expression in the POM, but by E11 this pattern began to diverge and by E15.5, the POM expressed predominantly *tcfap2 β* and very little *tcfap2 α* (Figure 6) (Bassett et al., 2012; Martino et al., 2016). Mice with germline deletions of the AP-2 β transcription factor (AP-2 β ^{-/-}) develop renal failure and die soon after birth and as a result, full eye development could not be examined. Thus, to circumvent the lethality of a germline deletion of the AP-2 β transcription factor, our laboratory employed the cre-loxP system to knockout the AP-2 β transcription factor exclusively in the craniofacial neural crest cells that contribute to the POM. Mice that were found to have a germline knockout of *tcfap2 β* from one allele and a functional deletion of *tcfap2 β* exclusive to the craniofacial neural crest cells from the second allele using the cre-loxP system are termed AP-2 β neural crest cell knockout mice (AP-2 β NCC KO) (Martino et al., 2016). The resulting phenotype of the AP-2 β NCC KO mice included a complete loss of the corneal endothelium and hyper-cellularization of the corneal stroma. Furthermore, closure of the iridocorneal angle was observed that was thought to be due to adhesion of the iris to the exposed corneal stroma. A complete, 360-degree, closure of the angle was confirmed using OCT, blocking AH drainage from the trabecular meshwork and uveoscleral pathways. This resulted in a closed-angle phenotype that produced an

increased IOP by three months of age. Furthermore, by two months of age, a significant decrease in the number of cells within the RGC layer was seen in flat-mount using neurobiotin injection as well as a significant decrease in *brn3a* labelled RGCs in paraffin sections at postnatal day 42. The AP-2 β NCC KO mouse also showed a decrease in the thickness of the IPL at postnatal day 42 and a decrease in the cross-sectional area of the optic nerve at two months. (Akula, Park, & West-Mays, 2019; Martino et al., 2016). Thus, not only does the AP-2 β NCC KO mouse show an increase in IOP and subsequent loss of RGCs but demonstrated this at a fraction of the time compared to other models. Since the conditional KO of AP-2 β is exclusive to the craniofacial NCC, it is expected that the neural retina, originating from the neural ectoderm, would be unaffected by the gene manipulation further indicating that the observed retinal damage is the result of increased IOP achieved by the closed-angle phenotype. Furthermore, embryonic expression AP-2 γ and AP-2 δ have been found in the GCL layer (Bassett et al., 2007), which is unaffected in our conditional knockout. However, to further confirm that the loss of RGCs and retinal damage is progressive an investigation of early postnatal stages is required. If the loss of RGCs is due to the increased IOP, an indication as to when the inflammation and first loss of RGCs occurs would give a time point as to when intervention should be administered.

Hypothesis and Research Aims

Rationale

50% of patients with Anterior Segmental Dysgenesis (ASD) will develop glaucoma as a result of the malformation of the aqueous humor draining structures. Our lab has shown that by disrupting the gene *tcfap2β* which codes for the transcription factor AP-2β exclusively in the neural crest cell-derived POM, we profoundly affected the development of the anterior segment. Specifically, removal of AP-2β caused the loss of the corneal endothelium and hyper-cellularization of the corneal stroma. The loss of the corneal endothelium likely contributed to the 360-degree adherence of the iris to the corneal stroma, resulting in a complete closure of the iridocorneal angle. Previously, our lab reported that the AP-2β NCC KO mouse could be a novel model for closed-angle glaucoma due to the fact that there is increased intraocular pressure at 3 months, decreased number of cells within the RGC layer at 2 months, decreased cross-sectional area of the optic nerve at 2 months, and a significant loss of brn3a labelled cells by P42. While promising, a key aspect of this model that remains to be shown is whether the loss of cells within the RGC layer was due to a developmental defect or due to the closed-angle phenotype. By investigating the number of cells within the RGC layer at early postnatal time points, we can identify if the decreased number of cells in the RGC layer as seen previously is developmental or due to the closed-angle phenotype. If the cell loss is found to occur before the closed-angle phenotype is present this would suggest that the deletion of the AP-2β transcription factor in the POM caused a developmental defect in the retina. If the cell loss is shown to be progressive and associated with the closed-angle phenotype, then it would further strengthen the plausibility of the AP-2β NCC KO mouse as an experimental model for glaucoma.

Furthermore, if the cell loss is deemed progressive investigation of early postnatal stages will allow us to identify the point in time at which we first start to see a statistical decrease in cells. This time point could be used in neuroprotective research as it serves as a benchmark for when potential neuroprotective drugs should be administered. This time point can be found by both looking for a statistically decrease in the number of cells within the RGC layer as well as the presence of neuroinflammatory markers.

Main Hypothesis

The loss of cells in the retinal ganglion cell layer described in the AP-2 β NCC KO mouse model is progressive, resulting from an increase in IOP.

Research Aims

Aim 1: To analyze and quantify the number of cells in the RGC layer at key postnatal days during retinal development.

To ensure that the decrease in cells within the retinal ganglion cell layer is not due to the conditional knockout of the *tcfap2 β* gene, it is important to examine whether there is a progressive loss of RGCs during the development of the retina at early postnatal stages in the AP-2 β NCC KO. Since the development of the retina continues after birth, the number of cells within the retinal ganglion cell layer will be quantified at postnatal stage days 4, 10, 35, and 40 to represent key time points in retinal development. Immunohistochemistry (IHC) will be used to quantify the number of cells within the RGC layer of the wild-type and AP-2 β NCC KO mice. If no differences in cell numbers are observed in the RGC cell layer at earlier postnatal stages, it will be proposed that the loss of RGC is progressive and that the AP-2 β NCC KO mouse is a

novel model for glaucoma. Furthermore, knowing at which stage the first difference in RGC number is observed between the wild-type and AP-2 β NCC KO will provide a time-point to target for future intervention.

Aim 2: To examine macroglial activity in AP-2 β NCC KO mice during retinal development.

To corroborate the decrease in the number of cells within the RGC layer with the presence of inflammation, it is crucial to understand how micro/macro glial cells are behaving at the postnatal stages of retinal development. Specifically, investigating at which point in time Müller cell-associated GFAP expression occurs. In the presence of neuroinflammation, Müller cells start to express GFAP and other intermediate filaments (Anderson et al 2008; Luna et al 2010) in an attempt to protect from further damage (Harada et al, 2003; Bringmann et al., 2006). IHC will be used to visualize the presence of Müller cell-expressed GFAP as it would suggest a time point that would indicate the start of neurodegeneration. If the loss of cells within the RGC layers occurs without Müller cells expressing GFAP, it could offer some insight as to the phenotype of the mouse model or the progression of the neurodegenerative disease. If the GFAP expression by Müller cells does not occur although the number of cells within the RGC layer decreases, it would suggest that that the subset of Müller cells that are thought to be derived from the NCC had been affected by the conditional knockout the AP-2 β transcription factor. Indicating that the AP-2 β transcription factor may have downstream effects on GFAP expression. If the GFAP expression by Müller cells does occur, either before or after the initial loss of cells within the RGC layer, it would offer a crucial time point at which researchers could administer interventions for study.

Methods

Animal Husbandry

All experiments were performed at McMaster University and animals were housed in the Central Animal Facility (CAF) in an SPF level room. Rooms were regulated to maintain a 22°C ambient temperature and a 12 hour light:dark cycle. Mouse cages were lined with dry bedding, while food (Harlan 8640 5% fat) and water was given *ad libitum*. All procedures were performed per the Animal Utility Protocol (AUP) submitted to the Animal Research Ethics Board (AREB).

Extraction and processing of tissue

Eyes

All eyes were extracted postmortem. Mice aged to postnatal day 4 and postnatal day 10 mice were decapitated, then eyes removed under a dissection microscope. Mice aged to postnatal day 35 and 40 had their eyes removed by cutting the optic nerve (ON) using curved scissors.

All eyes were immersed in a 4% paraformaldehyde-Sorensen's phosphate buffer for 2 hours then placed in 70% ethanol for 24 hours. Eyes were sent to the Histology Core lab at McMaster University to be processed for paraffin embedding (Paraplast Tissue Embedding Media, Fisher Scientific Waltham, MA).

Ears/Tails

All ear and tail tissue were extracted postmortem and used for DNA extraction. Tissue was stored at -20°C until DNA was extraction. DNA extraction was performed using the EZNA Tissue DNA Kit (Omega Bio-tek) and genotype was determined by established polymerase chain reaction (PCR) protocols.

PCR and Gel Electrophoresis

PCR and gel electrophoresis were performed for genotyping mice. PCR master mix recipes can be found in Table 1, 20µL of master mix was added to 5µL of DNA. Amplified DNA was run on 2% agarose gels for 60 minutes at a constant voltage of 120V. Tcfap2β primer combo was created by mixing 4µL of PGK PolyA DW, 4 exon Rev, and 4 exon DW primers. Wnt1cre primer was created by mixing 4µL of Cre1 and 4µL of Cre3 primers and diluting with 32µL of DNA/RNase free water. Primer sequences, PCR conditions, and product bands can be found in table 2.

Histology

Embedding and sectioning

Paraffin embedding was performed using a Leica EG 1150H embedding station. Eyes were positioned so the optical axis of the cornea was parallel to the horizontal horizon. Paraffin sections were cut on a Leica RM2255 microtome at a thickness of 4µm.

Immunohistochemistry

Paraffin-embedded sections were deparaffinized using three washes of xylene: 10 minutes, 15 minutes, 15 minutes; hydrated in serial ethanol solutions: 100% ethanol solution for 5 minutes (2x), 95% ethanol for 5 minutes, 70% ethanol for 5 minutes; then washed in water for 5 minutes. Antigen retrieval was performed by treating with 10 mM sodium citrate buffer (pH 6.0, boiling) for 20 minutes, then the same sodium citrate as it cooled for 20 minutes. All subsequent steps were performed in a humidifying chamber made by placing a damp paper towel in an empty slide box. 5% blocking solution

(normal serum of secondary antibody host) in 1XPBS + 0.1% tween20 was placed on sections and incubated for 1 hour at room temperature. Primary antibodies in 1% blocking solution were placed on sections and incubated at 4°C overnight. Secondary antibodies in 1.5% blocking serum were placed on sections and incubated at room temperature for 1 hour. Table 3 lists the antibodies and concentrations used for IHC experiments. Slides were mounted using ProLong Gold antifade reagent containing 4,6-diamino-2-phenylindole (DAPI) (Invitrogen – Molecular Probes, Burlington, Ontario) and visualized using a Leica CTR6 LED microscope with accompanying software (LAS X). Images were annotated with image editing software (GIMP).

Data Acquisition and Statistical Analysis

All mice were genotyped and only used if they were wild-type: two functional *tcfap2β* alleles, or AP-2B NCC KO: one *tcfap2β* deleted allele and one *tcfap2β* nulled allele by the cre-loxP system.

Brn3a labelled cells were counted manually in three regions of the retina: adjacent to the optic nerve head (denoted ONH), the approximate middle of the globe (denoted mid-periphery), and adjacent to the ciliary body (denoted periphery). A known length was measured in ImageJ and the number of pixels was calculated. Length of tissue calculated by the addition of the line segment lengths that were drawn along the tissue. The start and end of the length of tissue were defined by the first and last labeled cells that could be seen in the field of view. Vimentin and GFAP labelled cells were not quantified but instead defined as either present or not present. Three sections were quantified and averaged to be considered one sample.

Measurements were organized in Excel and imported into Prism for statistical analysis. Brn3a numbers were tested for significance with a 2-way independent ANOVAs for the three regions of the retina (independent variable: number of cells per length, dependent variables: age and phenotype). Data were considered significant when $p < 0.05$. When the ANOVA returned significant effectors, a Tukey multiple comparisons post-hoc test was performed.

Results

Quantification of Retinal Ganglion Cells at Early Postnatal Stages

Mice with genotypes that were shown to have both functional *tcfap2 β* alleles were termed Wild-type (WT) while mice with genotypes that were shown to be heterozygous for the knockout allele of *tcfap2 β* and a cre-mediated disruption of the remaining *tcfap2 β* allele were termed AP-2 β NCC KO (mutant). The presence of *tcfap2 β* and cre-recombinase alleles were detected through polymerase chain reaction (PCR) and gel electrophoresis. Figure 1 shows an example of the PCR and gel electrophoresis results used to determine the genotype. Two PCR experiments were performed to determine if the mutant genotype: one for the *wnt1cre* transgene (Cre1 and Cre3 primers) and another for the knocked out *tcfap2 β* allele (PGK-PolyA DW, 4 Exon Rev, and 4 Exon DW primers). Mice were identified as WT because they lacked the band denoting the *wnt1cre* transgene (420bp) and only had the mirrored *tcfap2 β* gene (220bp) (Figure 7A). Mice were identified as AP-2 β NCC KO mutants because they had the band denoting the *wnt1cre* transgene (420bp) as well as two distinct bands representing the two *tcfap2 β* alleles. The first band is the same as in the WT, the mirrored *tcfap2 β* gene (220bp) and the second band corresponding to the disrupted *tcfap2 β* gene (380bp) (Figure 7B). Mice that only presented with either the *wnt1cre* transgene or the two *tcfap2 β* allele disruptions, were deemed *wnt1cre^{+/-};**tcfap2 β ^{+/-loxP}* and *wnt1cre^{-/-};**tcfap2 β ^{-/-loxP}*, respectively. Mice with those phenotypes were not used as they contained one functional *tcfap2 β* allele. Immunohistochemistry (IHC) was performed on paraffin sections of eyes from WT and mutant mice. Since our lab had previously found a statistical decrease in the number of cells within the RGC layer between the mutant and WT littermates at 2 months of age (Martino et al.), we aimed to investigate earlier postnatal stages to reveal when the loss of cells first occurs.

Micrographs visualizing the expression of brn3a in mice at P4 are shown in figure 8. P4 represents the middle of the retinal remodeling stage at which the RGC layer is undergoing peak ganglion cell degeneration (Young, 1984). As a result, the RGC layer in both the WT and mutant mice was found to contain multiple layers of cells, particularly at the ONH and mid-periphery. No obvious difference in the number of brn3a positive cells was observed between the mutant and WT mice. To further confirm this, cell counts were performed in each region. In the WT, the average number of brn3a labelled cells was 93 ± 17 , 92 ± 7 , and 63 ± 13 (mean \pm standard deviation) cells per millimeter (cells/mm) of retinal tissue for the ONH, mid-periphery, and periphery regions respectively. In the mutant, the average number of brn3a labelled cells are 100 ± 9 , 79 ± 6 , and 56 ± 12 cells/mm of retinal tissue for the ONH, mid-periphery, and periphery respectively. No significant difference in the number of brn3a labelled cells between the WT and mutant littermates was found.

Brn3a expression in paraffin sections was also measured in mice aged to P10 at the ONH, mid-periphery, and periphery between WT and mutant phenotypes (Figure 9). P10 represents a time point at which retinal remodeling has already occurred and when the optic nerve is almost fully matured (Young, 1984). Since normal retinal remodeling has occurred at this stage, it is expected that the number of brn3a labelled cells will be much lower than that observed at P4, for both WT and mutant retinas. The average number of brn3a labelled cells in the WT was found to be 41 ± 25 , 31 ± 13 , and 27 ± 8 cells/mm for the ONH, mid-periphery, and periphery respectively, and in the mutant was found to be 60 ± 26 , 49 ± 12 , and 29 ± 5 cells/mm at the ONH, mid-periphery, and periphery respectively. A high degree of variability was seen at the level of the ONH in

both phenotypes and may be reflective of the remaining retinal remodeling between P4 and P10. Nonetheless, there was no significant difference found between the WT and mutant at P10. There was a significant decrease in the number of brn3a labelled cells between P4 and P10 in the WT mid-periphery and periphery, as well as a significant decrease between P4 and P10 in the mutant periphery. It was also observed that the standard deviations for the ONH region in both the WT and mutant phenotypes are similar in magnitude, suggesting that a similar degree of remodeling occurred in proximity to the optic nerve for both genotypes. Thus, the maturation of the optic nerve was still actively occurring at P10. In both phenotypes, the variability decreased in regions towards the periphery of the retina.

Brn3a expression in paraffin sections from mice at P35 of age was next measured (Figure 10). P35 represented a time point after the retina has fully matured. The number of brn3a labelled cells in the WT was found to be 45 ± 18 , 31 ± 5 , and 24 ± 4 cells/mm for the ONH, mid-periphery, and periphery respectively. For the mutant, the number of brn3a labelled cells was determined to be 28 ± 3 , 29 ± 5 , and 21 ± 4 cells/mm for the ONH, mid-periphery, and periphery respectively. Overall, we did not observe a significant difference between the WT and mutant. While the variability of mid-periphery and periphery in both phenotypes is of similar magnitude, the standard deviation between phenotypes at the ONH is not. Since the retina has fully matured, the standard deviation of the WT is representative of the natural biological variation of brn3a expressing cells at the ONH. Since the standard deviation of the mutant at the ONH dissimilar to that of the WT, P35 seems to be a time point of deviation of the mutant's phenotype from the WT.

Brn3a expression in paraffin sections was also measured in mice aged at P40 of age in the same regions as in previous time points (Figure 11). P40 may represent a time that damage could potentially affect the number of brn3a labelled cells in the mutant if the closed-angle phenotype causes glaucoma-like increases in IOP and subsequent retinal damage. P40 also represented a time point earlier than when our lab has previously seen a qualitative decrease in brn3a labelled cells in paraffin sections at P42 (Martino et al.). The number of brn3a labelled cells in the WT was found to be 64 ± 12 , 42 ± 11 , and 19 ± 1 cells/mm for the ONH, mid-periphery, and periphery respectively. The number of brn3a labelled cells in the mutant was 19 ± 25 , 11 ± 16 , and 4 ± 5 cells/mm for the ONH, mid-periphery, and periphery respectively. Although no significant difference between the mutant and WT was detected at P40, all regions of the retina the mutant exhibited a downward trend in brn3a labeled cells. Since P40 is the first time point where the standard deviation is greater than the mean in the mutant, P40 may be when we start to see a statistical decrease in brn3a labelled cells. Figure 12 is a bar graph summarizing the RGC cell count data from all time points and regions of the retina for both WT and mutant mice.

Based on the ANOVA results in tables 2, 3, and 4; it was determined that while phenotype was not a significant effector on the number of brn3a labelled cells in the three regions of the retina examined, age was a significant effector. Therefore, a Tukey multiple comparisons post-hoc test was performed to investigate if the loss of brn3a labelled cells was progressive with respect to age. Since P4 to P10 spans retinal remodeling, it would be expected that there would be a significant difference between the number of brn3a labelled cells at P4 and P10. As stated previously, in the WT a

significant decrease in brn3a labelled cells was found at the level of the mid-periphery and the periphery ($p=0.0006$ and $p=0.0047$, respectively) however not at the level of the ONH ($p=0.1649$). However, in the mutant the only statistical decrease is seen at the level of the periphery ($p=0.0478$) and not mid-periphery and ONH ($p=0.1695$ and $p=0.4193$, respectively). It is not known as to why the mid-peripheral region seems different between phenotypes; however, it should be recognized that optic nerve maturation may still be occurring which could contribute to the variability at P10. To investigate if the loss of brn3a labelled cells is progressive, a comparison between P10 to P40 within each phenotype was analyzed. Stepwise comparisons (P10 and P35, P35 and P40) were not appropriate because the glaucoma-like progression of RGC loss occurs over a relatively long amount of time. A comparison of subsequent time points could show no significant decrease, however, the sum of all decreases could prove to be significant. In the WT, it would be expected that the number of brn3a labelled cells should not significantly change post retinal remodeling and optic nerve maturation. The Tukey multiple comparisons test shows that in WT mice there is no significant decrease in brn3a labelled cells from P10 to P40 ($p=0.9003$, $p=0.9702$, and $p=0.9539$) at the ONH, mid-periphery, and periphery respectively. While the Tukey's multiple comparisons test shows no significant decrease between P10 and P40 in the mutant at the level of the ONH, it does show a significant decrease at the level of the mid-periphery and borderline significance at the level of the periphery ($p=0.4035$, $p=0.0406$, and $p=0.0618$). Together, these observations show that in the AP-2 β NCC KO model there is a subsequent loss of RGCs, which is progressive, which may mimic the loss that occurs in human glaucoma.

Expression of Glial Fibrillary Acidic Protein (GFAP) by Müller Cells

Glial Fibrillary Acidic Protein (GFAP) is an intermediate filament protein expressed by macroglia such as astrocytes, however in times of neuroinflammation Müller cells express GFAP in projections that span the entire retina. The purpose of examining GFAP expression in our mutant model at early postnatal stages was to corroborate the *brn3a* data with a marker for neuroinflammation. While Müller cells are responsible for protecting the neural retina by surrounding cells within the retina with vimentin, chronic expression of GFAP by Müller cells has been shown to have a positive effect on neurodegeneration (Bringmann et al., 2006; Coorey et al., 2012). When Müller cells express GFAP, the staining pattern contains projections that span the retina perpendicularly to the strata of the retina. Independent of inflammation, astrocytes constitutively express GFAP so astrocyte staining of GFAP was used as an internal positive control. The presence of GFAP by Müller cells was investigated for P4, P10, P35, and P40 in the three regions of the retina: ONH, mid-periphery, and periphery in both the WT and the mutant.

GFAP expression was first investigated in retinal sections at P4 to learn if neuroinflammation was already present in the retina in the mutant (Figure 13). As expected, no Müller cell GFAP expression was visualized in the WT, and no Müller cell-associated expression was present in the mutant as well. Concerning overall GFAP expression, at the level of the ONH and periphery, there was no qualitative difference between phenotypes. However, at the level of the mid-periphery in the mutant at P4, astrocyte expression of GFAP was detected and this was not seen in the WT (Figure 13).

GFAP expression was next investigated at P10 (Figure 14). Despite this time point being post-remodeling, there was no Müller cell-associated GFAP expression in either the WT or the mutant samples as shown by an absence in GFAP staining in projections traveling perpendicular to the retina strata. Astrocyte expression of GFAP appeared different between the phenotypes in all regions of the retina examined except for at the level of the ONH. In the mid-periphery and periphery regions of the WT retina, dull staining of astrocyte associated GFAP was observed, however within the same regions of the mutant retina the staining appeared brighter.

GFAP expression was next investigated in the P35 WT and mutant mouse phenotype to identify the presence of neuroinflammation (Figure 15). As expected in the WT, there was no Müller cell associated expression of GFAP as seen by the lack of visualized projections spanning the retina. However, in the mutant clear GFAP expression by Müller cells can be seen at the level of the ONH and periphery with minimal GFAP expression at the level of the mid-periphery. The expression of GFAP in Muller cells was not observed in the WT at this stage. This is an indication that neuroinflammation was occurring by P35 in the AP-2 β NCC KO mouse. While we did not detect a statistical difference between the number of brn3a labelled cells in the WT versus mutant at this postnatal stage, the increased GFAP expression preceded the RGC decrease that began to occur at P40.

In the P40 mutant, the Müller cell expression of GFAP increased in intensity across the three regions of the retina, while in comparison the P40 WT retina showed no Müller cell-associated expression of GFAP (Figure 16). In the mutant, the minimal Müller associated expression of GFAP at the level of the mid-periphery observed at

earlier stages had increased and the Müller cell expression of GFAP at the ONH and periphery remained consistent. This corresponds with the progressive loss of RGCs that seems to begin at postnatal day 40 further suggests that the retinal degeneration occurs gradually and exclusively after the retina has completed development. The GFAP visualization also corroborates the start of statistical loss of brn3a labelled cells being around P40 as the statistical decrease between P10 and P40 matches the presence of neuroinflammation as a result of neuronal death.

Müller Cell Expression of Vimentin in AP-2 β NCC KO mouse

Since Glial Fibrillary Acidic Protein (GFAP) is only expressed by Müller cells in the presence of neuroinflammation, it was important to ensure that the pattern of Müller cells was not altered in the AP-2 β NCC KO (mutant) versus wild-type (WT) mice. To visualize Müller cells, vimentin, an intermediate filament expressed by Müller cells, was stained using immunohistochemistry (IHC). It is expected that there should be little to no difference between the vimentin staining patterns between phenotypes, demonstrating that the presence of Müller cells is similar in the mutant as it is to the WT.

Vimentin expression in the postnatal days 4, 10, 35, and 40 in the WT and mutant mice was examined using IHC in the three regions of the retina examined: adjacent to the optic nerve (ONH), middle of the retina (mid-periphery), and adjacent to the ciliary body (periphery). In the three regions of the retina for postnatal days 4, 10, and 35 there was no difference in vimentin expression. However, vimentin expression in the postnatal day 40 mutant appears to be upregulated when compared to the postnatal day 40 WT (Figure 17), which is a sign of neurodegeneration (P. J. Anderson et al., 2008; Luna et al., 2010). To corroborate the increased vimentin expression with the presence of Müller cell-associated GFAP expression, colocalization of vimentin and

GFAP was performed on postnatal 40 WT and mutant mice. Figure 18 shows that there is exclusive colocalization of vimentin and GFAP in the inner nuclear layer and ganglion cell layer in WT mice, however, colocalization of vimentin and GFAP in the mutant extends to radially spanning the entire retina. The colocalization of the radially expressed GFAP with vimentin proves the presence of Müller cells in the mutant mouse and corroborates the fact that the radially expressed GFAP is expressed by Müller cells.

Discussion

Progressive Loss of Retinal Ganglion Cells in the AP-2 β NCC KO mouse

Previous work in our lab had suggested that the AP-2 β NCC KO mouse strain could be a potentially novel experimental model for glaucoma. Characteristics observed in this model such as increased intraocular pressure (IOP), loss of cells within the retinal ganglion cell (RGC) layer, and decreased optic nerve diameter are criteria that satisfy some important requirements for a model of glaucoma (Martino et al., 2016). However, one aspect that remained to be determined was whether the loss of cells in the RGC layer occurred progressively, over time, as is the case for glaucoma in humans. Thus, the overall goal of this thesis was to investigate the number of cells within the RGC layer in the AP-2 β NCC mutant at earlier postnatal stages to determine if the loss of cells observed previously is progressive and not due to a developmental defect that would be unrelated to closed-angle phenotype and the increased IOP.

Earlier work from our laboratory had shown that significant loss of cells in the RGC layer in the AP-2 β NCC mutant occurred at P42. Examination of RGC number at earlier stages of P4, P10, P35, and P40 was therefore carried out to determine when the loss of RGC is initiated. While we did not find a statistical difference between the mutant and wild-type (WT) controls in the three regions of the retina for all time points examined, we did observe a clear decreasing trend as we approached postnatal day 42, the original time point with a reported significant difference in RGC number.

Interestingly, at postnatal day 40, the variance in the number of RGC was greater than the calculated mean. This variability was attributed to the fact that some sections had zero brn3a labelled cells present in the three regions of the retina, while others had retained some. The complete lack of brn3a labelled cells was likely because a section was obtained from an area of the eye with more extensive RGC damage than others.

This is consistent with the progression of glaucoma as it is known that retinal damage glaucoma occurs segmentally. Ideally, flat mount sections may have prevented this variability and revealed more significant changes at this stage. However, flat mounts at such early stages are not possible to obtain and we, therefore, had to rely on serial sections.

It was also observed that age had a significant effect on the number of retinal ganglion cells in both phenotypes examined, mutants and control littermates. This finding is to be expected since mouse retinal progenitor cells undergo a pruning process involving programmed cell death (Young, 1984) until postnatal day 21. Thus, any data from retinas before postnatal day 21 should capture the effect of age on the decline in the number of brn3a labelled cells.

When comparing the P10 to P40 pair between both phenotypes, no significant difference between P10 and P40 was found for the WT and a significant difference for the AP-2 β NCC KO ($p=0.9702$ and $p=0.0406$, respectively) which strongly suggests that the loss of brn3a labelled cells is progressive and indicative of glaucoma. What this shows is that in the WT littermate controls, the amount of RGC death over 30 days was significantly lower than in the AP-2 β NCC KO mouse. It is expected that some loss of RGCs would be observed from P10 to P21 as this is still within the developmental pruning of the RGC layer, however in the WT that loss was not significant. In comparison, in the mutant, the number of RGCs that died during the same period was significant. This finding indicates that another mechanism, other than the developmental pruning rate alone is contributing to the loss of RGC during that time. That mechanism that is likely contributing to the increased rate of RGC death in the mutant is the closure

of the iridocorneal angle leading to increased IOP, which causes mechanical stress of the RGC layer and subsequent increased rate of RGC death in the AP-2 β NCC KO mutant when compared to WT littermate controls.

The fact that RGC loss is occurring in the AP-2 β NCC KO mouse is extremely important as this would further demonstrate that it is a useful experimental model for glaucoma. One important benefit of this model is the amount of time needed for obtaining significant results. Other models such as the DBA/2J model, do not exhibit a significant loss of RGCs until 11 to 15 months, whereas the AP-2 β NCC KO model shows a significant degree of retinal ganglion cell death by 42 days. As a result, the AP-2 β NCC KO mouse strain requires less time and resources as a model of glaucoma since experiments can be completed in a shorter time frame. The closed-angle phenotype in the AP-2 β NCC KO mouse model was found to be highly penetrant; each AP-2 β NCC KO mouse had complete adherence of the iris to the corneal stroma. Therefore, each mouse presents with the same 360-degree closed-angle phenotype, causing complete closure of both the classical and uveoscleral aqueous humor drainage pathways that result in a similar loss of RGC between each mutant mouse. This is in contrast to the DBA/2J mouse where the increased IOP is based on the iris stroma deposition and subsequent blockage of the aqueous humor drainage structures. Since the deposition is highly variable, so is the increase in IOP and subsequent loss of retinal ganglion cells. As a result, many more DBA/2J mice need to be examined to obtain significant findings. Furthermore, the consistency of the AP-2 β NCC KO mouse progression means that intervention experimentation can be standardized. Rather than performing interventional surgery or administration of potentially neuroprotectant drugs

on a mouse model with a highly variable baseline, all interventions can be given on a mouse with a well-defined disease state as a function of age. In the AP-2 β NCC KO mouse, the drug can be administered much earlier, for example, day 25, and all mice will have a similar degree of intraocular pressure due to the mechanism of aqueous humor blockage being virtually identical between mice. Both the drastically shorter wait time and mechanism consistency shown in the AP-2 β NCC KO mouse are crucial qualities in a glaucoma model and could be a great benefit to glaucoma research.

GFAP expression by Müller cells marks neuroinflammation at P35 to P40

One drawback to investigating the number of brn3a labelled cells in sections rather than whole-mount preparations is that there is a potential to underestimate the degree of damage within the retina. Thus, we utilized another way to corroborate the brn3a data, by investigating GFAP expression. Overexpression of GFAP by Müller cells, also known as gliosis, is an indication of neuroinflammation that is also hypothesized to exacerbate retinal degeneration if chronic (Bringmann et al., 2006; Coorey et al., 2012). Thus, by visualizing GFAP expression in Müller cells, we can corroborate the brn3a data and further support the progressive loss of RGCs in the mutant. While the expression of GFAP was not observed at earlier postnatal stages of both the WT and mutant, it became visible with an increase in age exclusively in the mutant. Müller cell expression of GFAP was initially observed at postnatal day 35 and increased through postnatal day 40 and postnatal day 42 in the mutant while no Müller cell expression of GFAP was observed in the WT littermates. This coincided with the brn3a data for both the WT and mutant phenotypes. The loss of RGCs as demonstrated by the brn3a data and the presence of Müller associated GFAP expression indicates that the decreasing trend of brn3a labelled cells occurs in the presence of neuroinflammation in the mutant,

while the lack of RGC loss and Müller cell GFAP expression in the WT indicates that neither RGC loss nor neuroinflammation is occurring in the WT. This further supports the progressive nature of the retinal ganglion cell loss in the AP-2 β NCC KO mouse as RGC loss and GFAP expression by Müller cells is seen exclusively in the mutant phenotype. Currently, the data suggests that the Müller cell expression of GFAP precedes the statistical decrease in the number of RGCs, supporting the concept that GFAP expression by Müller cells may have been initiated to protect from mechanical damage to the RGC layer. However, it is unclear as to if by P40 the expression of GFAP is contributing to the loss of RGCs as in the case of chronic gliosis (Bringmann et al., 2006; Coorey et al., 2012). Although the *brn3a* data revealed that damage to the retinal ganglion cell layer was first observed at postnatal day 40, we are not certain as to when it was initiated. Segmental loss of cells within the retinal ganglion cell layer may have occurred at earlier stages and we did not detect it using serial sectioning. Thus, some damage to the retina may have occurred earlier than Müller cell expression of GFAP. However, our data has suggested that Müller cells are expressing GFAP before a statistical decrease in RGC number is observed in serial sections. This could either mean that loss of RGCs is earlier than P42 as previously reported, or that Müller cell expression of GFAP could be an indication of impending degeneration rather than an indication that degeneration has occurred. If GFAP expression by Müller cells drastically precedes retinal damage, it could suggest that the administration of neuroprotectant drugs would need to be at an even earlier time than Müller cells expressing GFAP would originally suggest to prevent loss of RGCs. Regardless of how much time separates retinal degeneration and GFAP expression, it will indicate when

neuroprotectant drugs should be administered and when Müller cells are reacting to the retinal degeneration. Furthermore, since it is hypothesized that chronic gliosis exacerbates retinal degeneration if we find evidence that suggests that Müller cell expression of GFAP is contributing to the loss of RGCs then-new drug targets that reduce GFAPs contribution to retinal degeneration could be investigated.

Vimentin expression confirms the presence of Müller cells in AP-2 β NCC KO mouse

Glial cells are primarily derived from the neural tube, however, it was hypothesized that a subset of Müller cells are derived from cranial neural crest cells (Liu et al., 2013). Since our knockout of AP-2 β is exclusive to the NCC, there is the potential for genetic manipulation to affect Müller cells. Therefore, it was crucial to prove that Müller cell numbers in the retina were unaffected without using GFAP expression. By visualizing vimentin, no difference between phenotypes at postnatal stages 4, 10, and 35 was found. This suggests that the Müller cell population was unaffected as a result of the AP-2 β NCC KO. Furthermore, the colocalization of GFAP and vimentin confirms that the GFAP expression was by Müller cells and the increased expression of vimentin at postnatal day 40 confirms that despite the knockout of AP-2 β from the cranial NCCs, the Müller cells are responding appropriately to retinal degeneration and exhibiting classic signs of gliosis (P. J. Anderson et al., 2008; Luna et al., 2010). While the presence of Müller cells seems to be unaffected, the degree of vimentin expression appeared decreased in the AP-2 β NCC KO mouse. Quantification of vimentin expression using western blot band intensity would help to determine if the vimentin expression is significantly affected by the AP-2 β NCC KO. Since the role of vimentin is to mechanically protect the cells in the retinal ganglion cell layer, the decrease in

vimentin expression in the AP-2 β NCC KO mouse may have helped in facilitating retinal degeneration.

Conclusions and Future Directions

This study has shown that within the AP-2 β NCC KO mouse strain, the loss of retinal ganglion cells by P42 is not a result of the disruption of the AP-2 β transcription factor causing a genetic defect in retinal development. The evidence suggesting that the closed-angle phenotype created by the adherence of the iris to the corneal stroma and subsequent increased IOP contributes to retinal degeneration similar to human glaucoma includes segmental loss of retinal ganglion cells, decreased number of cells within the RGC layer, and decreased optic nerve diameter (Martino et al., 2016). This evidence is strengthened by the results presented in the thesis. The decreasing trend of RGCs suggesting a progressive nature to the retinal degeneration as well as the corroboration of GFAP expression by Müller cells exclusively in the AP-2 β NCC KO mutant at P35 and P40 suggesting that the retinal damage occurs over time. The combination of these findings indicates that the AP-2 β NCC KO could be an important asset to experimental glaucoma research. This experimental model is the only strain of mouse that has a profound effect on the uveoscleral outflow pathway. All other models, genetic and physically induced, exclusively decrease aqueous humor drainage via the conventional pathway, which in mice, only contributes to 20% of overall aqueous humor outflow (Aihara et al., 2003a; Fautsch & Johnson, 2006). Since the AP-2 β NCC KO mouse model completely blocks the uveoscleral pathway, it is an extremely powerful experimental model for glaucoma. Although significance was not found at P40, it was likely due fact that there is some variability in the amount of damage to the retina during early stages, which minimizes by 2-3 months of age.

Further experimentation of the AP-2 β NCC KO mouse strain itself should focus on standardization of the model and optimization of model use such as experiments that

further the understanding of how the model presents. While this thesis focused on *brn3a* positive cells for visualizing cell numbers in the RGC layer, antibodies against RNA-binding protein with multiple splicing (RBPMS) have been shown to reliably and exclusively visualize RGCs and was not investigated (Rodriguez, de Sevilla Müller, & Brecha, 2014). By investigating similar stages as *brn3a* with RBPMS and generating a similar understanding of how the number of RBPMS positive cells changes over time, it would increase the robustness of the model as researchers would not be required to use *brn3a* for visualization of the RGC layer. RBPMS and *brn3a* co-localization has shown that while all *brn3a* expressing cells also express RBPMS, approximately 80% of RBPMS expressing cells also express *brn3a* (Rodriguez et al., 2014). Not only will investigating similar stages as *brn3a* with RBPMS give a more complete idea of how RGC populations are changing in the mutant over time, it may also show discrepancies in how the RGC layer presents throughout progression of degeneration based on the target for visualization. If the discrepancy between *brn3a* and RBPMS is found to grow as the disease in the mutant progresses, it would suggest that select populations of RGCs have variable susceptibility to mechanical injury than others, similar to the more injury-resistant characteristics seen in melanopsin-expressing RGCs (Li et al., 2006). In addition to the use of RBPMS in serial sections, flat-mount experiments using both *brn3a* and RBPMS should be done between P21 and P35. Although it has been shown that RGC numbers can be accurately estimated in serial sections (Fileta et al., 2008; Mead et al., 2014), one disadvantage to using serial sections was the potential to miss regions of the retina that may be damaged. While this thesis shows that loss of RGCs can be observed by P42 in serial sections, the precision of when RGC loss is occurring

is extremely important in neuroprotectant experiments. By P21, the development of the eye is essentially complete and flat mounts experiments become much more viable. By investigating both *brn3a* and RBPMS staining in flat-mount between P21 and P35, a tighter timeframe of when retinal degeneration is initiated can be found. Once this tighter timeframe is reported, a standardized drug administration time can be chosen and the legitimacy of neuroprotectant experiments will increase as all neuroprotectants will be able to be compared in a more standardized manner. The highest degree of precision could be realized by using Fluorescence-activated cell sorting (FACS) to count individual cells. Although the organization of RGC loss in glaucoma is segmental and since that segmentation has already been shown, the experiments could be reduced purely to the number of RGCs by using FACS for even higher precision and high-throughput.

Furthermore, serial section experiments visualizing GFAP and quantifying GFAP expression by western blot intensity can be done within the tighter timeframe to investigate Müller cell-expressed GFAP's role. As previously discussed, Müller cell expression of GFAP is theorized to have both protective and degenerative effects if chronic expression occurs. By investigating the relationship between the initiation of retinal degeneration and Müller cell expression of GFAP, it could lead to new research questions ranging from the mechanism of GFAP associated protection or degeneration to developing new drugs that either increase the protective component of GFAP or antagonize the degenerative component.

Another experiment that could be done is quantifying the amount of vimentin present in the AP-2 β NCC KO mutant. The amount of vimentin seemed to be lower

within the mutant when compared to WT littermates, which could contribute to the RGC loss. Since vimentin is an IF that protects RGCs from mechanical stress, if the amount of vimentin is decreased as measured by western blot intensity analysis in the mutant, then that could be a reason as to why RGC loss occurs so quickly.

Finally, another experiment that could be performed is to surgically recreate an aqueous humor drainage system in the AP-2 β NCC KO mouse by performing a selective laser trabeculoplasty (SLT) procedure and prove the effect of increased intraocular pressure on RGC loss, as SLTs have shown to be effective in reducing IOP in closed-angle glaucoma (Ho et al., 2009). Due to 360-degree adherence of the iris to the exposed corneal stroma, it is hypothesized that aqueous humor drainage is completely blocked. While it is unknown, and probably unlikely, that 100% of the aqueous humor drainage is prevented in the mutant, re-establishing an aqueous humor drainage system may alleviate the mechanical stress caused by the increased IOP. In the absence of increased IOP, the loss of RGCs in the AP-2 β NCC KO mutant should become absent. This would strongly suggest that increased IOP is more than just a risk factor for glaucoma, but also a cause of mechanical stress that induces RGC death.

References

- Aihara, M., Lindsey, J. D., & Weinreb, R. N. (2003a). Aqueous humor dynamics in mice. *Investigative Ophthalmology & Visual Science*, *44*(12), 5168–5173. <https://doi.org/10.1167/iovs.03-0504>
- Aihara, M., Lindsey, J. D., & Weinreb, R. N. (2003b). Ocular Hypertension in Mice with a Targeted Type I Collagen Mutation. *Investigative Ophthalmology & Visual Science*, *44*(4), 1581–1585. <https://doi.org/10.1167/iovs.02-0759>
- Akula, M., Park, J. W., & West-Mays, J. A. (2019). Relationship between neural crest cell specification and rare ocular diseases. *Journal of Neuroscience Research*, *97*(1), 7–15. <https://doi.org/10.1002/jnr.24245>
- Anderson, M. G., Smith, R. S., Hawes, N. L., Zabaleta, A., Chang, B., Wiggs, J. L., & John, S. W. M. (2002). Mutations in genes encoding melanosomal proteins cause pigmentary glaucoma in DBA/2J mice. *Nature Genetics*, *30*(1), 81–85. <https://doi.org/10.1038/ng794>
- Anderson, P. J., Watts, H., Hille, C., Philpott, K., Clark, P., Gentleman, M. C. S., & Jen, L.-S. (2008). Glial and endothelial blood-retinal barrier responses to amyloid-beta in the neural retina of the rat. *Clinical Ophthalmology (Auckland, N.Z.)*, *2*(4), 801–816.
- Araie, M., Sekine, M., Suzuki, Y., & Koseki, N. (1994). Factors contributing to the progression of visual field damage in eyes with normal-tension glaucoma. *Ophthalmology*, *101*(8), 1440–1444.
- Ascher, K. W. (1954). [Veins of the aqueous humor in glaucoma]. *Bollettino D'oculistica*, *33*(3), 129–144.
- Badea, T. C., Cahill, H., Ecker, J., Hattar, S., & Nathans, J. (2009). Distinct roles of transcription factors Brn3a and Brn3b in controlling the development, morphology, and function of retinal ganglion cells. *Neuron*, *61*(6), 852–864. <https://doi.org/10.1016/j.neuron.2009.01.020>
- Bassett, E. A., Korol, A., Deschamps, P. A., Buettner, R., Wallace, V. A., Williams, T., & West-Mays, J. A. (2012). Overlapping expression patterns and redundant roles for AP-2 transcription factors in the developing mammalian retina. *Developmental Dynamics: An Official Publication of the American Association of Anatomists*, *241*(4), 814–829. <https://doi.org/10.1002/dvdy.23762>
- Bassett, E. A., Pontoriero, G. F., Feng, W., Marquardt, T., Fini, M. E., Williams, T., & West-Mays, J. A. (2007). Conditional Deletion of Activating Protein 2 α (AP-2 α) in the Developing Retina Demonstrates Non-Cell-Autonomous Roles for AP-2 α in Optic Cup Development. *Molecular and Cellular Biology*, *27*(21), 7497–7510. <https://doi.org/10.1128/MCB.00687-07>
- Bharti, K., Nguyen, M.-T. T., Skuntz, S., Bertuzzi, S., & Arnheiter, H. (2006). The other pigment cell: Specification and development of the pigmented epithelium of the vertebrate eye. *Pigment Cell Research*, *19*(5), 380–394. <https://doi.org/10.1111/j.1600-0749.2006.00318.x>
- Bill, A., & Hellsing, K. (1965). Production and drainage of aqueous humor in the cynomolgus monkey (*Macaca irus*). *Investigative Ophthalmology*, *4*(5), 920–926.
- Bill, A., & Svedbergh, B. (1972). Scanning electron microscopic studies of the trabecular meshwork and the canal of Schlemm—An attempt to localize the main resistance to outflow of aqueous humor in man. *Acta Ophthalmologica*, *50*(3), 295–320.

- Bok, D. (1993). The retinal pigment epithelium: A versatile partner in vision. *Journal of Cell Science. Supplement*, 17, 189–195.
- Boland, M. V., & Quigley, H. A. (2007). Risk factors and open-angle glaucoma: Classification and application. *Journal of Glaucoma*, 16(4), 406–418. <https://doi.org/10.1097/IJG.0b013e31806540a1>
- Bringmann, A., Grosche, A., Pannicke, T., & Reichenbach, A. (2013). GABA and Glutamate Uptake and Metabolism in Retinal Glial (Müller) Cells. *Frontiers in Endocrinology*, 4, 48. <https://doi.org/10.3389/fendo.2013.00048>
- Bringmann, A., Pannicke, T., Grosche, J., Francke, M., Wiedemann, P., Skatchkov, S. N., ... Reichenbach, A. (2006). Müller cells in the healthy and diseased retina. *Progress in Retinal and Eye Research*, 25(4), 397–424. <https://doi.org/10.1016/j.preteyeres.2006.05.003>
- Brubaker, R. F. (2001). Measurement of uveoscleral outflow in humans. *Journal of Glaucoma*, 10(5 Suppl 1), S45-48.
- Chang, E. E., & Goldberg, J. L. (2012). Glaucoma 2.0: Neuroprotection, neuroregeneration, neuroenhancement. *Ophthalmology*, 119(5), 979–986. <https://doi.org/10.1016/j.optha.2011.11.003>
- Chong, R. S., & Martin, K. R. (2015). Glial cell interactions and glaucoma. *Current Opinion in Ophthalmology*, 26(2), 73–77. <https://doi.org/10.1097/ICU.0000000000000125>
- Chow, R. L., & Lang, R. A. (2001). Early eye development in vertebrates. *Annual Review of Cell and Developmental Biology*, 17, 255–296. <https://doi.org/10.1146/annurev.cellbio.17.1.255>
- Coleman, A. L., & Miglior, S. (2008). Risk factors for glaucoma onset and progression. *Survey of Ophthalmology*, 53 Suppl1, S3-10. <https://doi.org/10.1016/j.survophthal.2008.08.006>
- Coorey, N. J., Shen, W., Chung, S. H., Zhu, L., & Gillies, M. C. (2012). The role of glia in retinal vascular disease. *Clinical & Experimental Optometry*, 95(3), 266–281. <https://doi.org/10.1111/j.1444-0938.2012.00741.x>
- Cvekl, A., & Tamm, E. R. (2004). Anterior eye development and ocular mesenchyme. *BioEssays : News and Reviews in Molecular, Cellular and Developmental Biology*, 26(4), 374–386. <https://doi.org/10.1002/bies.20009>
- Erkman, L., McEvilly, R. J., Luo, L., Ryan, A. K., Hooshmand, F., O'Connell, S. M., ... Rosenfeld, M. G. (1996). Role of transcription factors Brn-3.1 and Brn-3.2 in auditory and visual system development. *Nature*, 381(6583), 603–606. <https://doi.org/10.1038/381603a0>
- Fautsch, M. P., & Johnson, D. H. (2006). Aqueous Humor Outflow. *Investigative Ophthalmology & Visual Science*, 47(10), 4181–4187. <https://doi.org/10.1167/iovs.06-0830>
- Fileta, J. B., Huang, W., Kwon, G. P., Filippopoulos, T., Ben, Y., Dobberfuhr, A., & Grosskreutz, C. L. (2008). Efficient Estimation of Retinal Ganglion Cell Number: A Stereological Approach. *Journal of Neuroscience Methods*, 170(1), 1–8. <https://doi.org/10.1016/j.jneumeth.2007.12.008>
- Franze, K., Grosche, J., Skatchkov, S. N., Schinkinger, S., Foja, C., Schild, D., ... Guck, J. (2007). Muller cells are living optical fibers in the vertebrate retina.

- Proceedings of the National Academy of Sciences of the United States of America*, 104(20), 8287–8292. <https://doi.org/10.1073/pnas.0611180104>
- Gage, P. J., Rhoades, W., Prucka, S. K., & Hjalt, T. (2005). Fate maps of neural crest and mesoderm in the mammalian eye. *Investigative Ophthalmology & Visual Science*, 46(11), 4200–4208. <https://doi.org/10.1167/iovs.05-0691>
- Goel, M., Picciani, R. G., Lee, R. K., & Bhattacharya, S. K. (2010). Aqueous Humor Dynamics: A Review. *The Open Ophthalmology Journal*, 4, 52–59. <https://doi.org/10.2174/1874364101004010052>
- Goldmann, H. (1950). [Minute volume of the aqueous in the anterior chamber of the human eye in normal state and in primary glaucoma]. *Ophthalmologica. Journal International D'ophtalmologie. International Journal of Ophthalmology. Zeitschrift Fur Augenheilkunde*, 120(1–2), 19–21. <https://doi.org/10.1159/000300856>
- Gould, D. B., & John, S. W. M. (2002). Anterior segment dysgenesis and the developmental glaucomas are complex traits. *Human Molecular Genetics*, 11(10), 1185–1193. <https://doi.org/10.1093/hmg/11.10.1185>
- Gould, D. B., Smith, R. S., & John, S. W. M. (2004). Anterior segment development relevant to glaucoma. *The International Journal of Developmental Biology*, 48(8–9), 1015–1029. <https://doi.org/10.1387/ijdb.041865dg>
- Grierson, I., & Lee, W. R. (1978). Pressure effects on flow channels in the lining endothelium of Schlemm's canal. A quantitative study by transmission electron microscopy. *Acta Ophthalmologica*, 56(6), 935–952.
- Hayhow, W. R., Sefton, A., & Webb, C. (1962). Primary optic centers of the rat in relation to the terminal distribution of the crossed and uncrossed optic nerve fibers. *The Journal of Comparative Neurology*, 118, 295–321.
- Hickey, T. L., & Spear, P. D. (1976). Retinogeniculate projections in hooded and albino rats: An autoradiographic study. *Experimental Brain Research*, 24(5), 523–529.
- Ho, C. L., Lai, J. S. M., Aquino, M. V., Rojanapongpun, P., Wong, H. T., Aquino, M. C., ... Barkana, Y. (2009). Selective laser trabeculoplasty for primary angle closure with persistently elevated intraocular pressure after iridotomy. *Journal of Glaucoma*, 18(7), 563–566. <https://doi.org/10.1097/IJG.0b013e318193c2d1>
- John, S. W., Smith, R. S., Savinova, O. V., Hawes, N. L., Chang, B., Turnbull, D., ... Heckenlively, J. R. (1998). Essential iris atrophy, pigment dispersion, and glaucoma in DBA/2J mice. *Investigative Ophthalmology & Visual Science*, 39(6), 951–962.
- Johnstone, M. A., & Grant, W. G. (1973). Pressure-dependent changes in structures of the aqueous outflow system of human and monkey eyes. *American Journal of Ophthalmology*, 75(3), 365–383.
- Li, R. S., Chen, B.-Y., Tay, D. K., Chan, H. H. L., Pu, M.-L., & So, K.-F. (2006). Melanopsin-expressing retinal ganglion cells are more injury-resistant in a chronic ocular hypertension model. *Investigative Ophthalmology & Visual Science*, 47(7), 2951–2958. <https://doi.org/10.1167/iovs.05-1295>
- Libby, R. T., Anderson, M. G., Pang, I.-H., Robinson, Z. H., Savinova, O. V., Cosma, I. M., ... John, S. W. M. (2005). Inherited glaucoma in DBA/2J mice: Pertinent disease features for studying the neurodegeneration. *Visual Neuroscience*, 22(5), 637–648. <https://doi.org/10.1017/S0952523805225130>

- Liu, B., Hunter, D. J., Rooker, S., Chan, A., Paulus, Y. M., Leucht, P., ... Helms, J. A. (2013). Wnt signaling promotes Müller cell proliferation and survival after injury. *Investigative Ophthalmology & Visual Science*, *54*(1), 444–453. <https://doi.org/10.1167/iovs.12-10774>
- Luna, G., Lewis, G. P., Banna, C. D., Skalli, O., & Fisher, S. K. (2010). Expression profiles of nestin and synemin in reactive astrocytes and Müller cells following retinal injury: A comparison with glial fibrillar acidic protein and vimentin. *Molecular Vision*, *16*, 2511–2523.
- Lundkvist, A., Reichenbach, A., Betsholtz, C., Carmeliet, P., Wolburg, H., & Pekny, M. (2004). Under stress, the absence of intermediate filaments from Müller cells in the retina has structural and functional consequences. *Journal of Cell Science*, *117*(16), 3481–3488. <https://doi.org/10.1242/jcs.01221>
- M, K. (2015). Present and New Treatment Strategies in the Management of Glaucoma. *The Open Ophthalmology Journal*, *9*, 89–100. <https://doi.org/10.2174/1874364101509010089>
- Mandal, A. K., & Chakrabarti, D. (2011). Update on congenital glaucoma. *Indian Journal of Ophthalmology*, *59*(Suppl1), S148–S157. <https://doi.org/10.4103/0301-4738.73683>
- Marquardt, T. (2003). Transcriptional control of neuronal diversification in the retina. *Progress in Retinal and Eye Research*, *22*(5), 567–577.
- Martínez-Morales, J. R., Rodrigo, I., & Bovolenta, P. (2004). Eye development: A view from the retina pigmented epithelium. *BioEssays: News and Reviews in Molecular, Cellular and Developmental Biology*, *26*(7), 766–777. <https://doi.org/10.1002/bies.20064>
- Martino, V. B., Sabljic, T., Deschamps, P., Green, R. M., Akula, M., Peacock, E., ... West-Mays, J. A. (2016). Conditional deletion of AP-2 β in mouse cranial neural crest results in anterior segment dysgenesis and early-onset glaucoma. *Disease Models & Mechanisms*, *9*(8), 849–861. <https://doi.org/10.1242/dmm.025262>
- Mason, C. A., Sparrow, N., & Lincoln, D. W. (1977). Structural features of the retinohypothalamic projection in the rat during normal development. *Brain Research*, *132*, 141–148. [https://doi.org/10.1016/0006-8993\(77\)90711-9](https://doi.org/10.1016/0006-8993(77)90711-9)
- Mead, B., Thompson, A., Scheven, B. A., Logan, A., Berry, M., & Leadbeater, W. (2014). Comparative Evaluation of Methods for Estimating Retinal Ganglion Cell Loss in Retinal Sections and Wholemounts. *PLOS ONE*, *9*(10), e110612. <https://doi.org/10.1371/journal.pone.0110612>
- Quigley, H. A., & Broman, A. T. (2006). The number of people with glaucoma worldwide in 2010 and 2020. *British Journal of Ophthalmology*, *90*(3), 262–267. <https://doi.org/10.1136/bjo.2005.081224>
- Quigley, H. A., McKinnon, S. J., Zack, D. J., Pease, M. E., Kerrigan-Baumrind, L. A., Kerrigan, D. F., & Mitchell, R. S. (2000). Retrograde axonal transport of BDNF in retinal ganglion cells is blocked by acute IOP elevation in rats. *Investigative Ophthalmology & Visual Science*, *41*(11), 3460–3466.
- Rodriguez, A. R., de Sevilla Müller, L. P., & Brecha, N. C. (2014). The RNA binding protein RBPMS is a selective marker of ganglion cells in the mammalian retina. *The Journal of Comparative Neurology*, *522*(6), 1411–1443. <https://doi.org/10.1002/cne.23521>

- Satoda, M., Zhao, F., Diaz, G. A., Burn, J., Goodship, J., Davidson, H. R., ... Gelb, B. D. (2000). Mutations in TFAP2B cause Char syndrome, a familial form of patent ductus arteriosus. *Nature Genetics*, 25(1), 42–46. <https://doi.org/10.1038/75578>
- Senatorov, V., Malyukova, I., Fariss, R., Wawrousek, E. F., Swaminathan, S., Sharan, S. K., & Tomarev, S. (2006). Expression of mutated mouse myocilin induces open-angle glaucoma in transgenic mice. *The Journal of Neuroscience: The Official Journal of the Society for Neuroscience*, 26(46), 11903–11914. <https://doi.org/10.1523/JNEUROSCI.3020-06.2006>
- Tham, Y.-C., Li, X., Wong, T. Y., Quigley, H. A., Aung, T., & Cheng, C.-Y. (2014). Global prevalence of glaucoma and projections of glaucoma burden through 2040: A systematic review and meta-analysis. *Ophthalmology*, 121(11), 2081–2090. <https://doi.org/10.1016/j.ophtha.2014.05.013>
- Wang, S. W., Mu, X., Bowers, W. J., Kim, D.-S., Plas, D. J., Crair, M. C., ... Klein, W. H. (2002). Brn3b/Brn3c double knockout mice reveal an unsuspected role for Brn3c in retinal ganglion cell axon outgrowth. *Development (Cambridge, England)*, 129(2), 467–477.
- Xiang, M., Zhou, L., Macke, J. P., Yoshioka, T., Hendry, S. H., Eddy, R. L., ... Nathans, J. (1995). The Brn-3 family of POU-domain factors: Primary structure, binding specificity, and expression in subsets of retinal ganglion cells and somatosensory neurons. *The Journal of Neuroscience: The Official Journal of the Society for Neuroscience*, 15(7 Pt 1), 4762–4785.
- Young, R. W. (1984). Cell death during differentiation of the retina in the mouse. *The Journal of Comparative Neurology*, 229(3), 362–373. <https://doi.org/10.1002/cne.902290307>
- Zhang, X., Serb, J. M., & Greenlee, M. H. W. (2011). Mouse retinal development: A dark horse model for systems biology research. *Bioinformatics and Biology Insights*, 5, 99–113. <https://doi.org/10.4137/BBI.S6930>

Figures

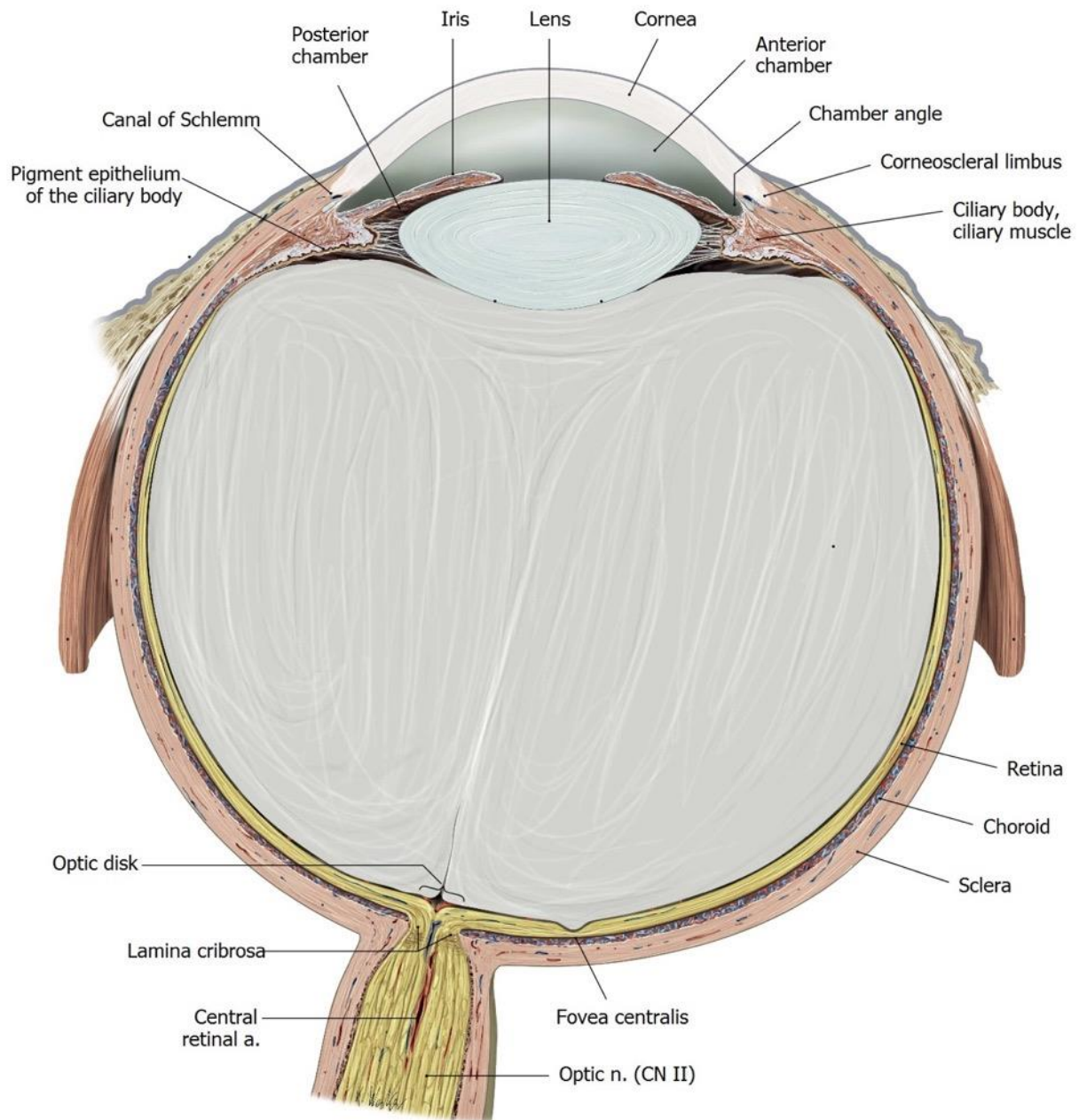


Figure 1: General Anatomy of the Mammalian Eye. A schematic depicting the anatomical structures of the mammalian eye. Adapted from Thieme Atlas of Anatomy, 3rd Edition, 2019)

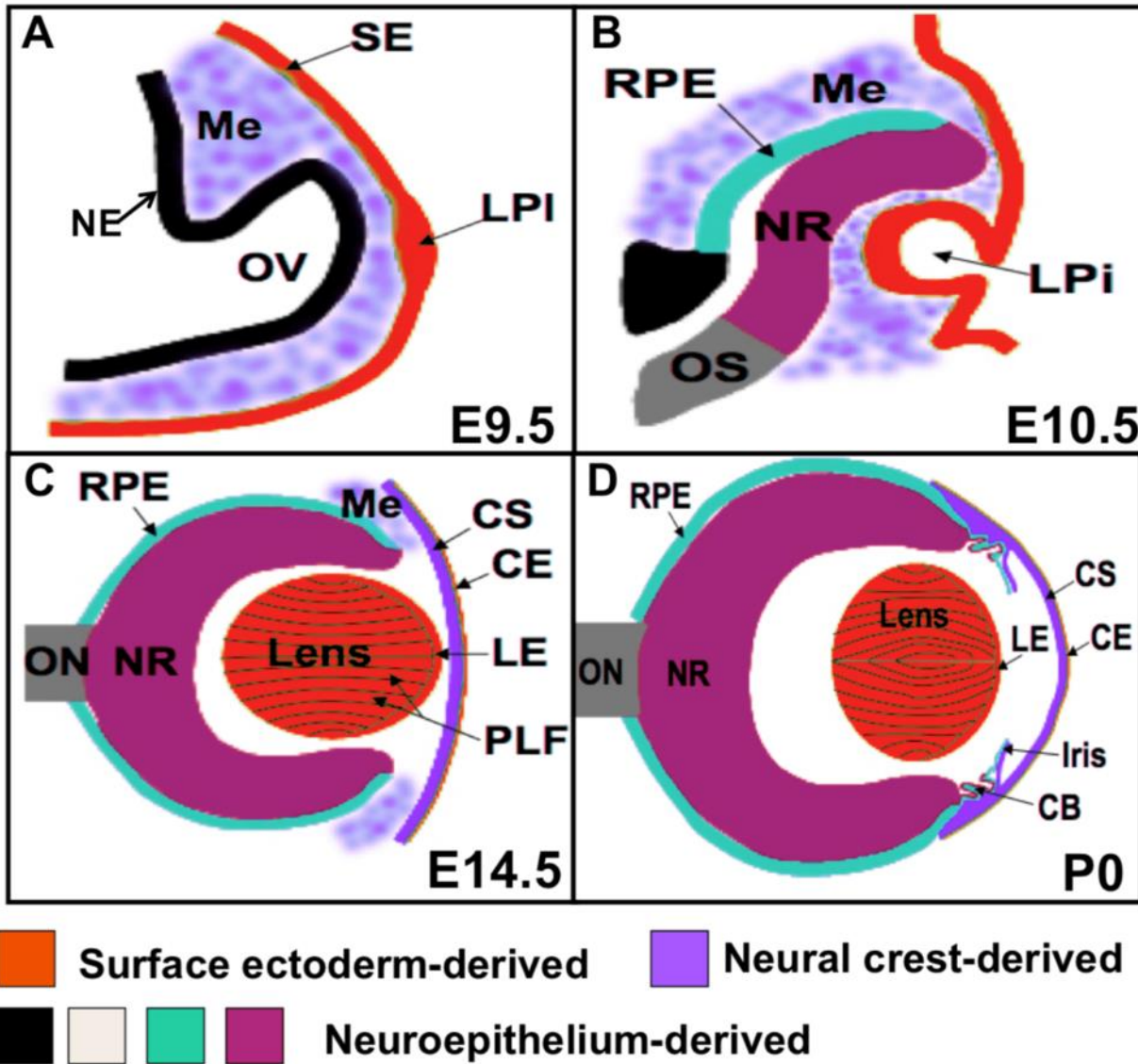


Figure 2: Vertebrate eye development and tissue derivations. Schematic of the stages of eye development including formation of the optic vesicle (A), formation of the lens pit (B), detachment of the lens (C), and formation of ciliary body and corneal epithelium (D). NE: neuroepithelium, Me: periocular mesenchyme, SE: surface ectoderm, OV: optic vesicle, LPi: lens pit, OS: optic stock, CE: corneal epithelium, CS: corneal stroma, NR: neural retina, RPE: retinal pigmented epithelium, LE: lens epithelium, PLF: proliferating lens fibers, CB: ciliary body, ON: optic nerve. (Adapted from Bassett, E.A, 2012).

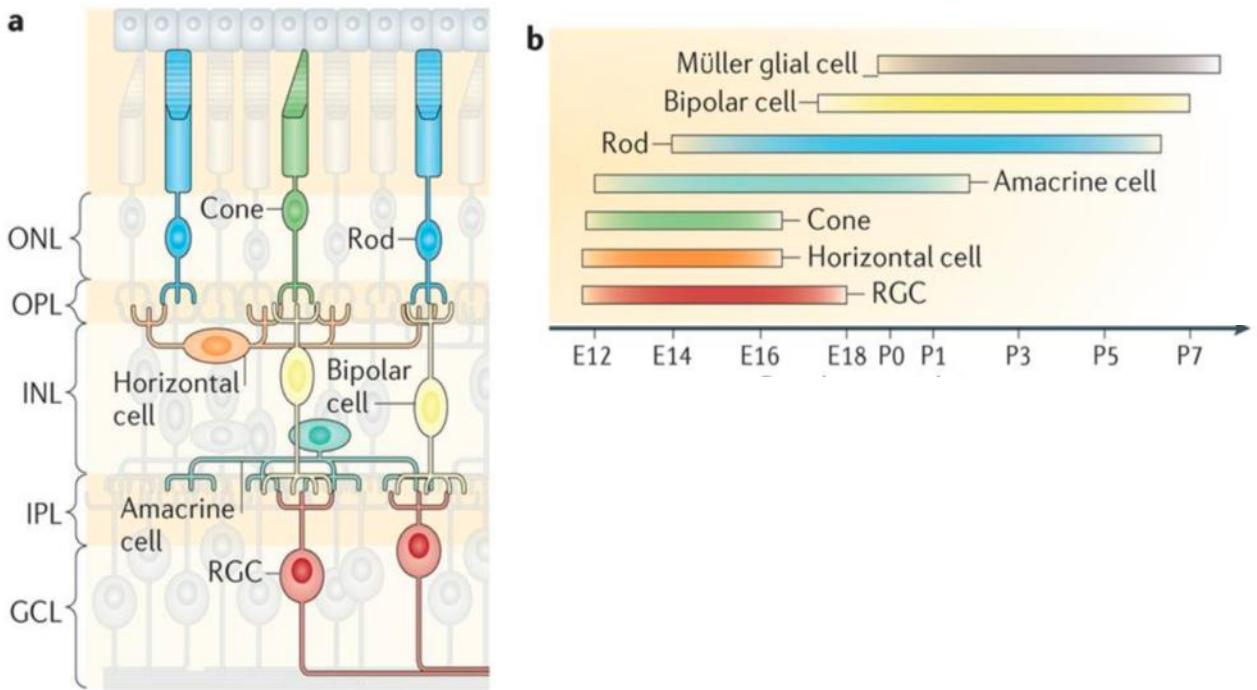


Figure 3: Retinal development. Schematic showing the three distinct layers of the retina (A) and the chronological order that neurons are born. ONL: outer nuclear layer, INL: inner nuclear layer, GCL: ganglion cell layer, OPL: outer plexiform layer, IPL: inner plexiform layer. (Adapted from Cepko, 2014)

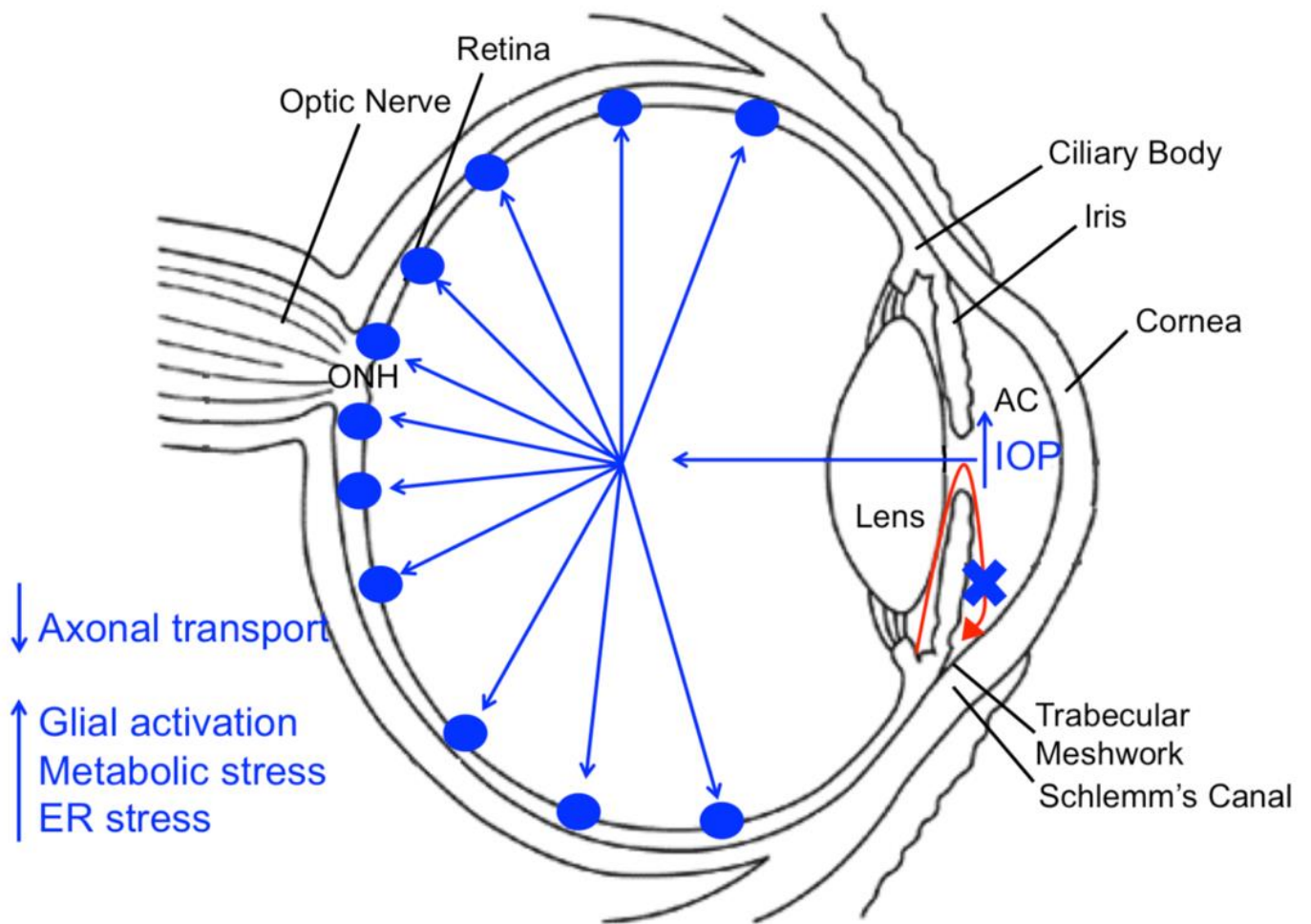


Figure 4: Schematic showing the theory of the relationship between increased intraocular pressure and glaucoma. Impediment of the aqueous humor outflow (red arrow and blue X) happens, the pressure within the anterior chamber increases. The increased pressure transfers to the retina and compresses at the optic nerve head (ONH). Compression of the retina results in decreased retrograde axonal transport of trophic factors and/or increased glial, metabolism, and ER stress. (Adapted from Martino et al., 2016).

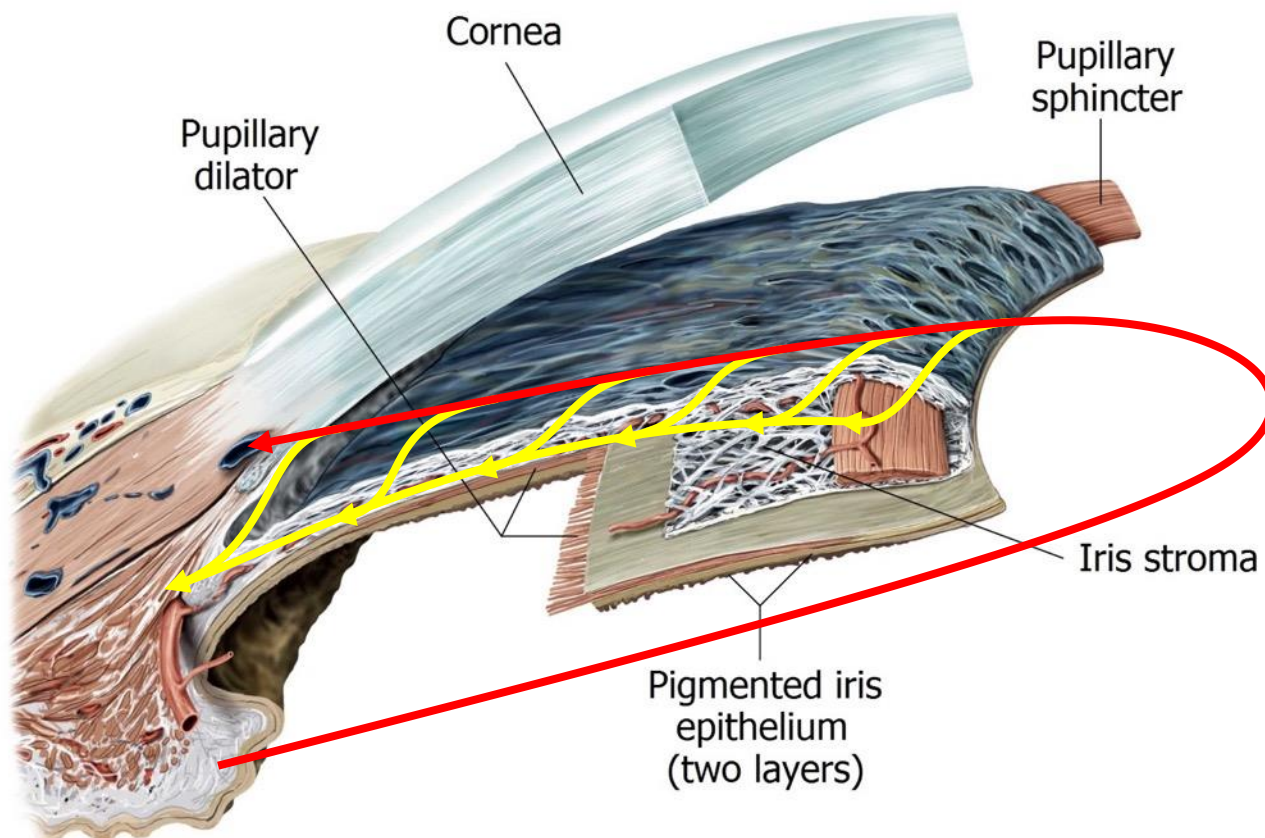


Figure 5: Anterior Chamber and Aqueous Humor Pathways. Schematic depicting the anatomical structures of the anterior segment. Aqueous humor is produced by the ciliary body, travels between the lens and iris to enter the anterior chamber. Aqueous humor continues to the iridocorneal angle where it will drain via the trabecular meshwork and Schlemm's canal (red arrow) or the uveoscleral pathway (yellow arrow). When these drainage pathways are disrupted, intraocular pressure increases and could lead to glaucoma-like symptoms. (Adapted from Thieme of Anatomy, 3rd edition, 2019)

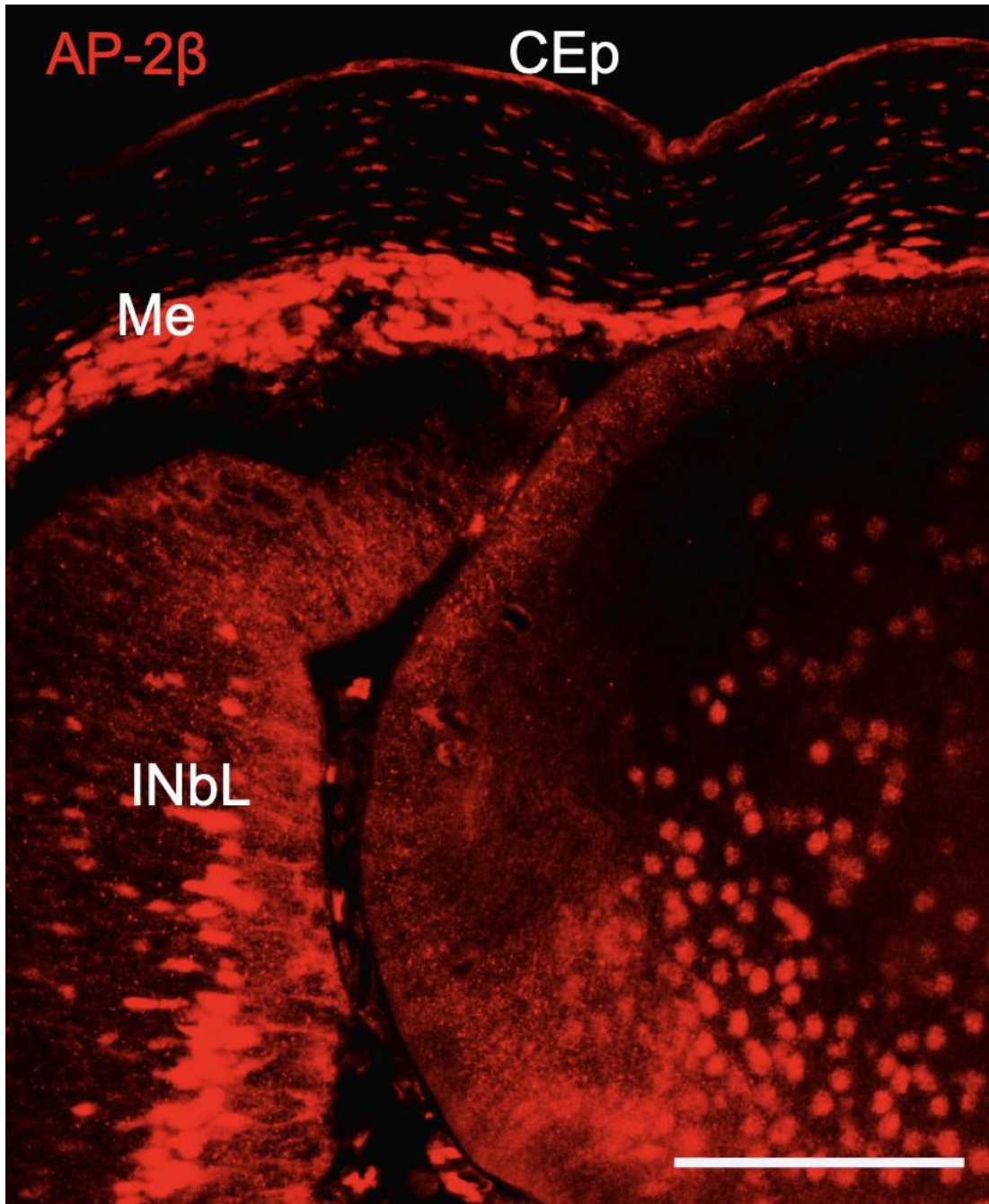
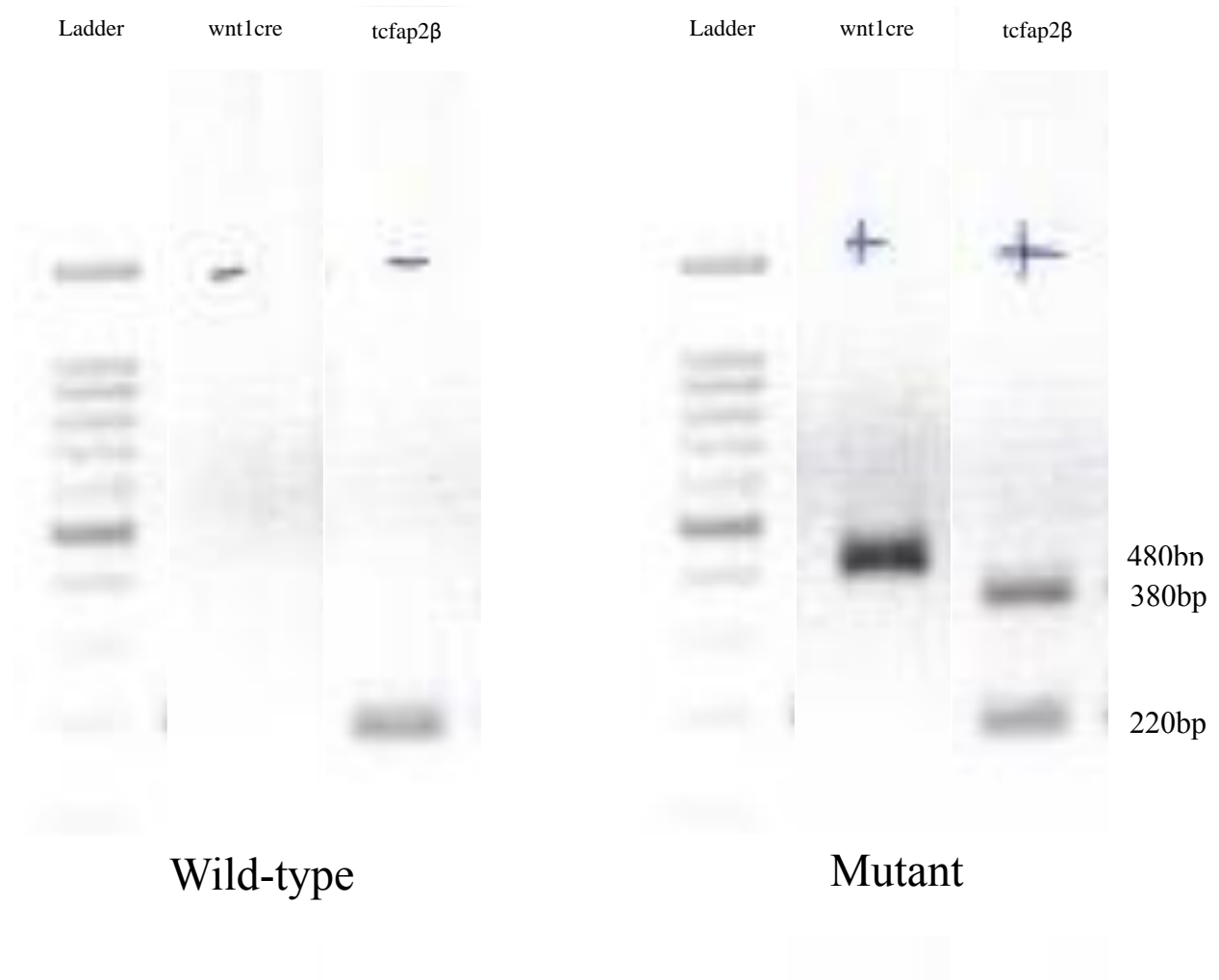


Figure 6: The expression of AP-2 β in an E15.5 murine eye. AP-2B expression was shown to in the corneal epithelium (Cep), the developing corneal stroma (CS), the inner neuroblast layer (INbL), and the periocular mesenchyme (Me). Scalebars set to 100 μ m (Adapted from Martino et al., 2016).

ANODE



CATHODE

Figure 7: PCR results denoting mouse genotype. Two PCR experiments were used to confirm wild-type (WT) versus AP-2 β NCC KO (mutant) mice: *wnt1cre* transgene and two disrupted *tcfap2 β* alleles. 100bp DNA ladder was used.

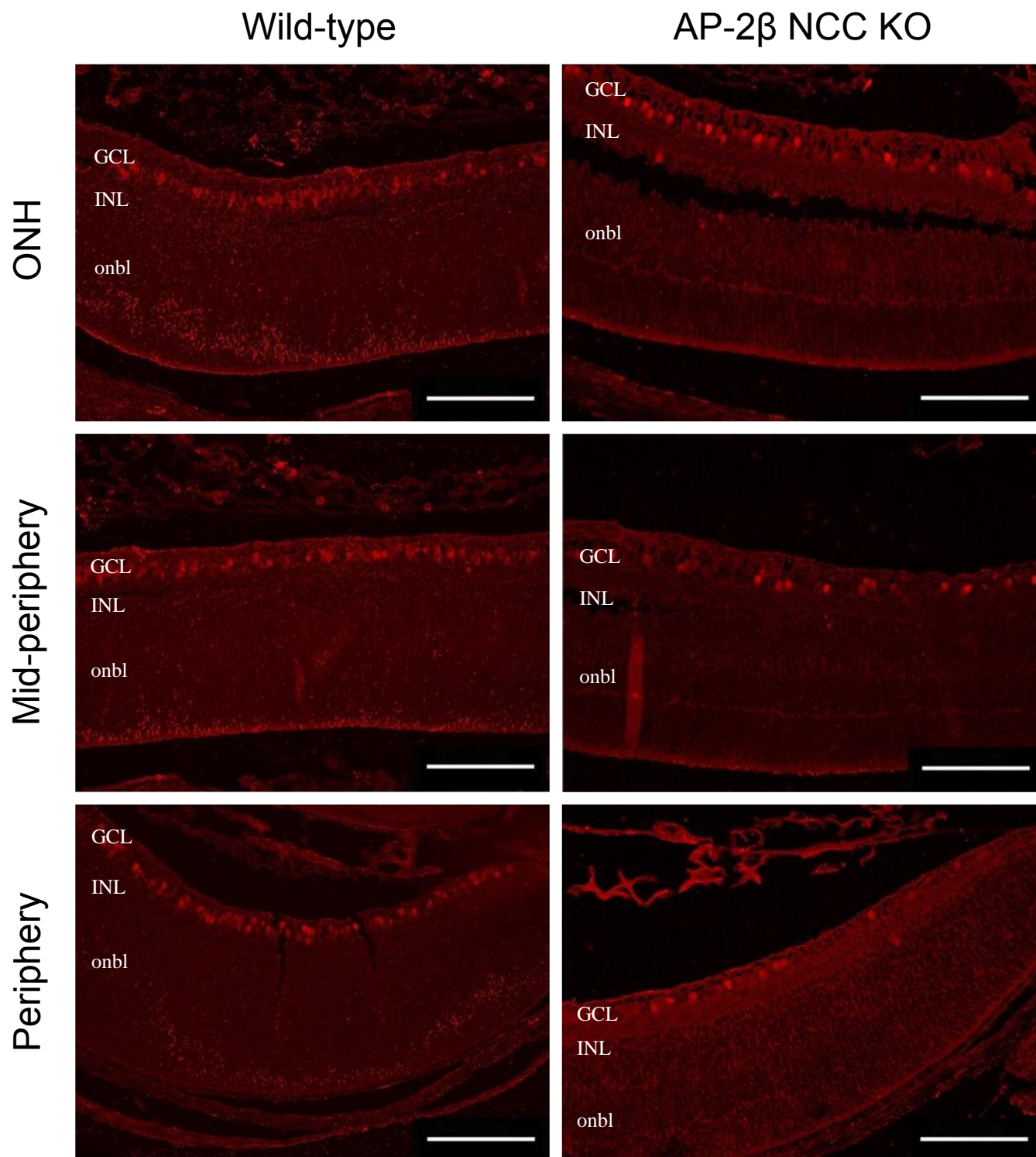


Figure 8: Brn3a expression in postnatal day 4 wild-type and AP-2β NCC KO. Brn3a (red) in the wild-type and AP-2β NCC KO retina. ONH represents the retina adjacent to the Optic nerve, mid-periphery represents the middle of the retina, and the periphery represents the retina adjacent to the ciliary body. Ganglion Cell Layer (GCL), Inner Nuclear Layer (INL), Outer Neuroblast Layer (onbl). Scale bars: 100 μ m

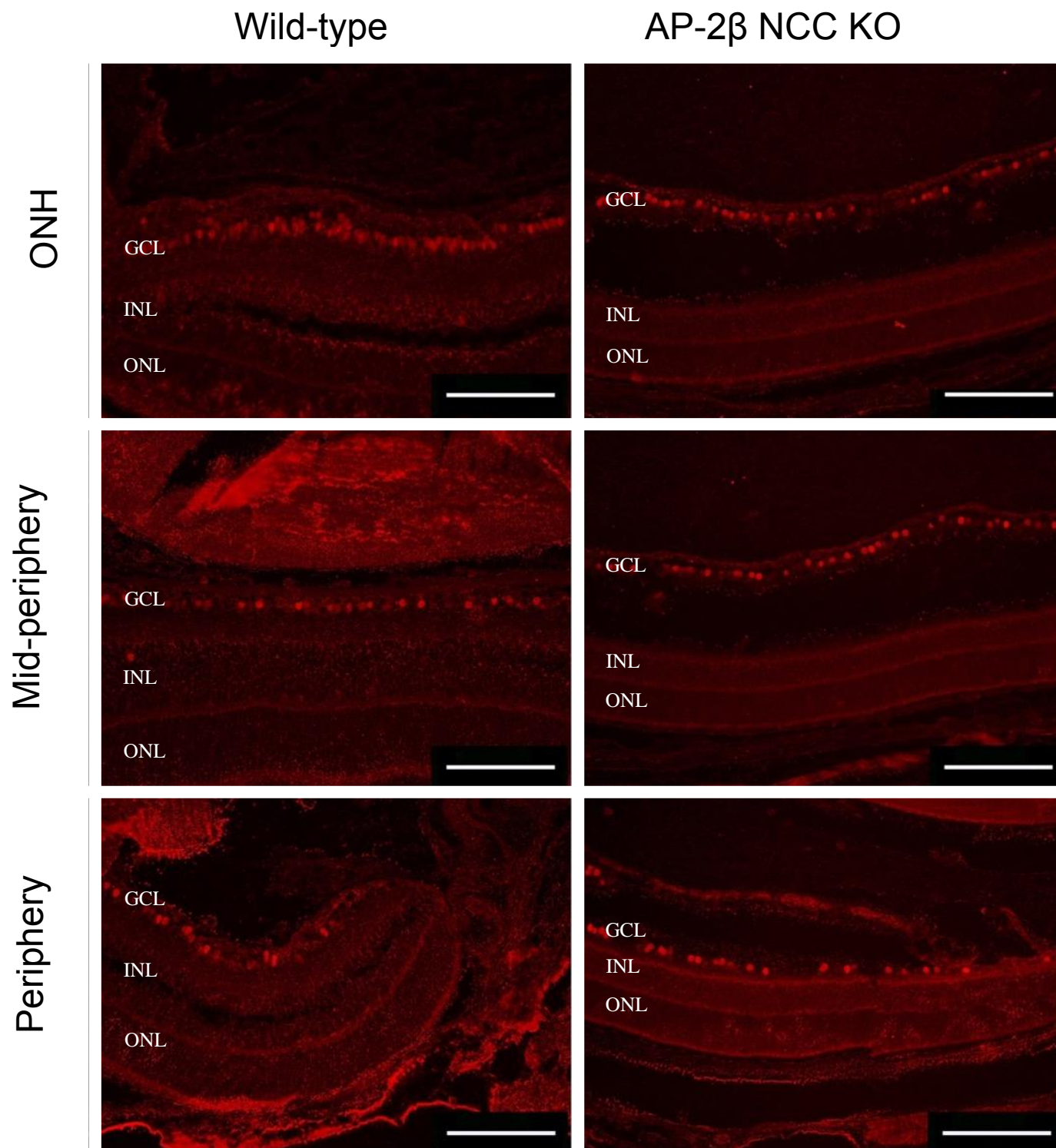


Figure 9: Brn3a expression in postnatal day 10 wild-type and AP-2β NCC KO. Brn3a (red) in the wild-type and AP-2β NCC KO retina. ONH represents the retina adjacent to the Optic nerve, mid-periphery represents the middle of the retina, and the periphery represents the retina adjacent to the ciliary body. Ganglion Cell Layer (GCL), Inner Nuclear Layer (INL), Outer Nuclear Layer (ONL). Scale bars: 100 μ m

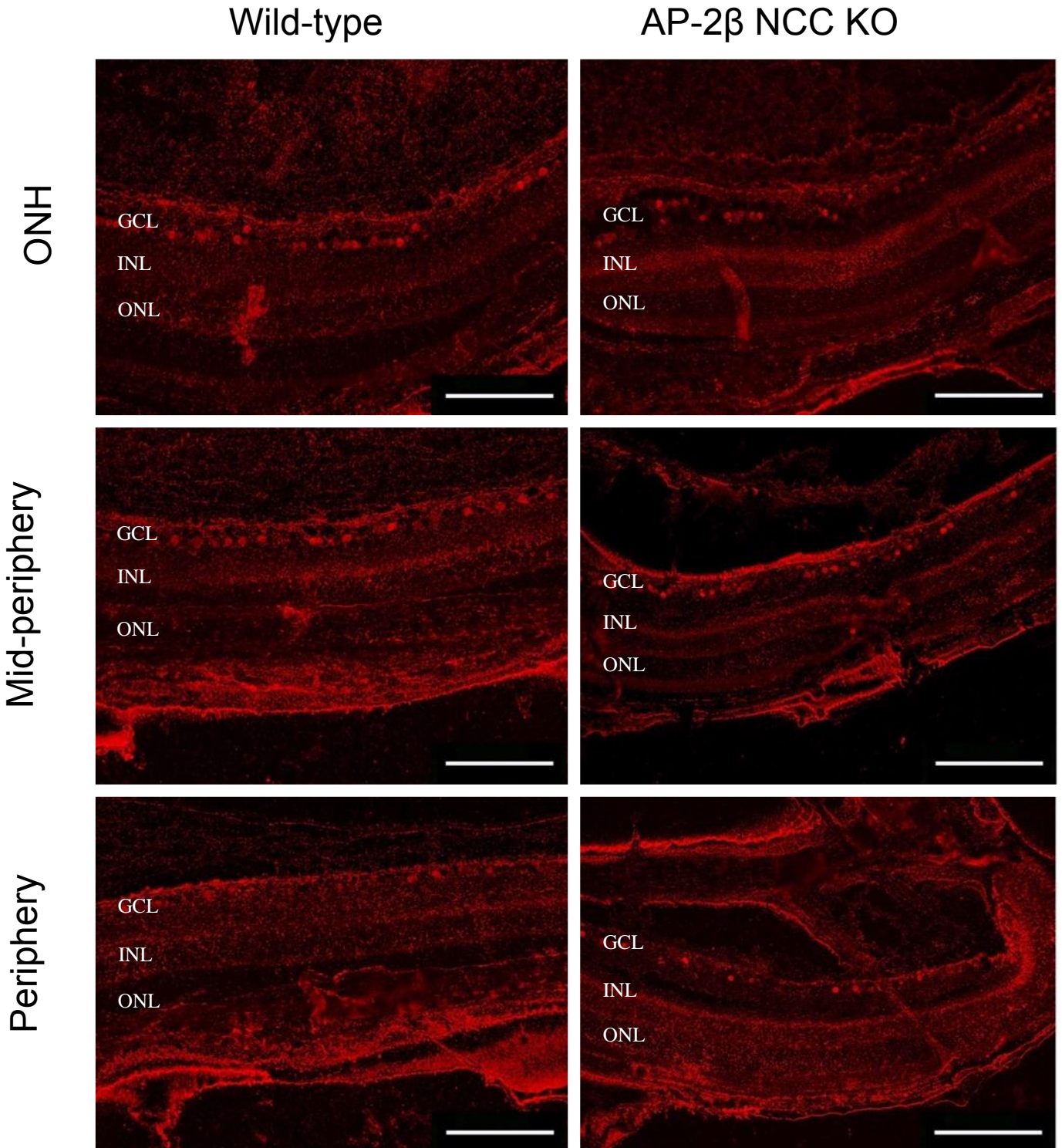


Figure 10: Brn3a expression in postnatal day 35 wild-type and AP-2β NCC KO. Brn3a (red) in the wild-type and AP-2β NCC KO retina. ONH represents the retina adjacent to the Optic nerve, mid-periphery represents the middle of the retina, and the periphery represents the retina adjacent to the ciliary body. Ganglion Cell Layer (GCL), Inner Nuclear Layer (INL), Outer Nuclear Layer (ONL). Scale bars: 100 μm

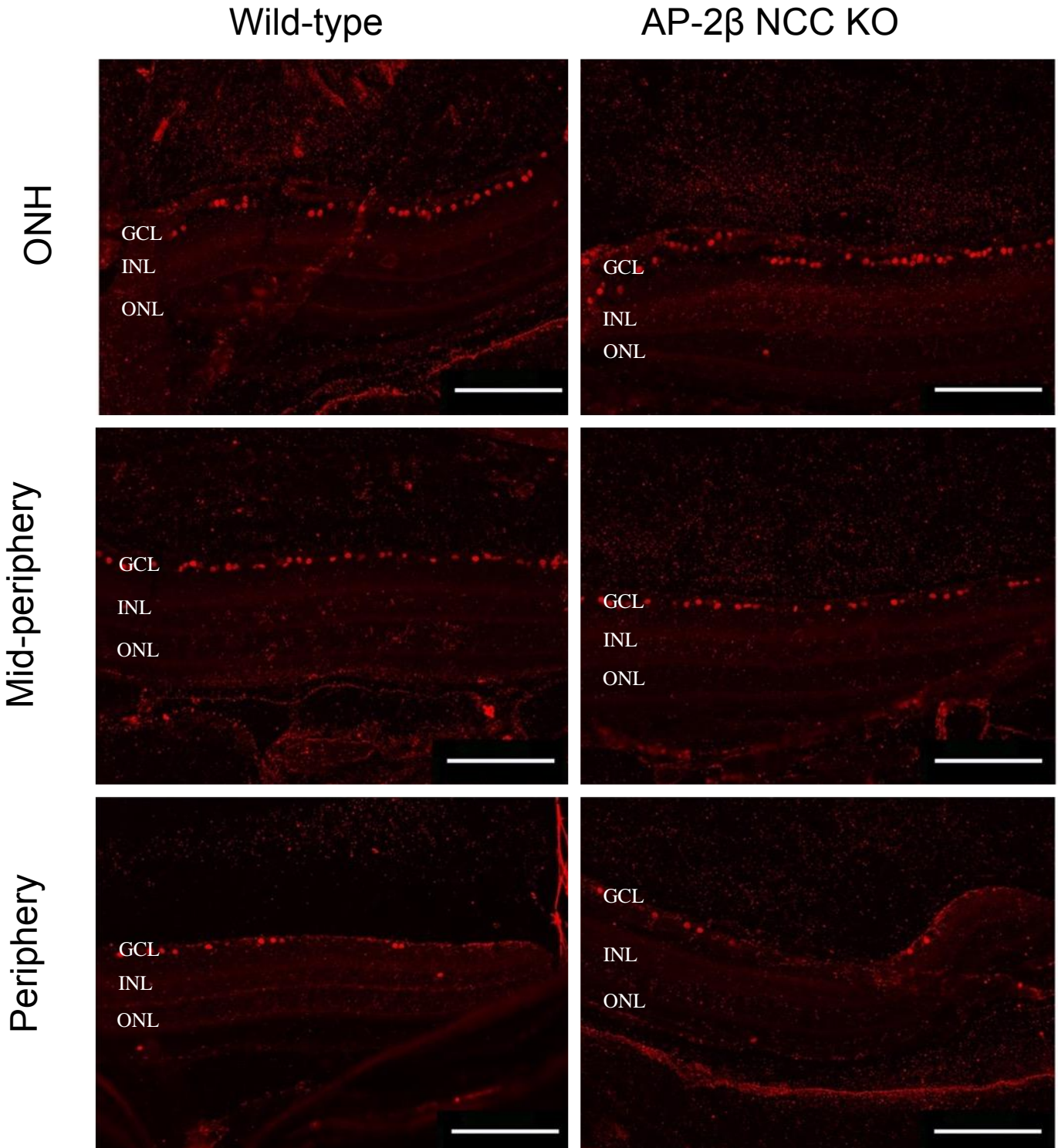


Figure 11: *Brn3a* expression in postnatal day 40 wild-type and AP-2β NCC KO. *Brn3a* (red) in the wild-type and AP-2β NCC KO retina. ONH represents the retina adjacent to the Optic nerve, mid-periphery represents the middle of the retina, and the periphery represents the retina adjacent to the ciliary body. Ganglion Cell Layer (GCL), Inner Nuclear Layer (INL), Outer Nuclear Layer (ONL). Scale bars: 100 μm

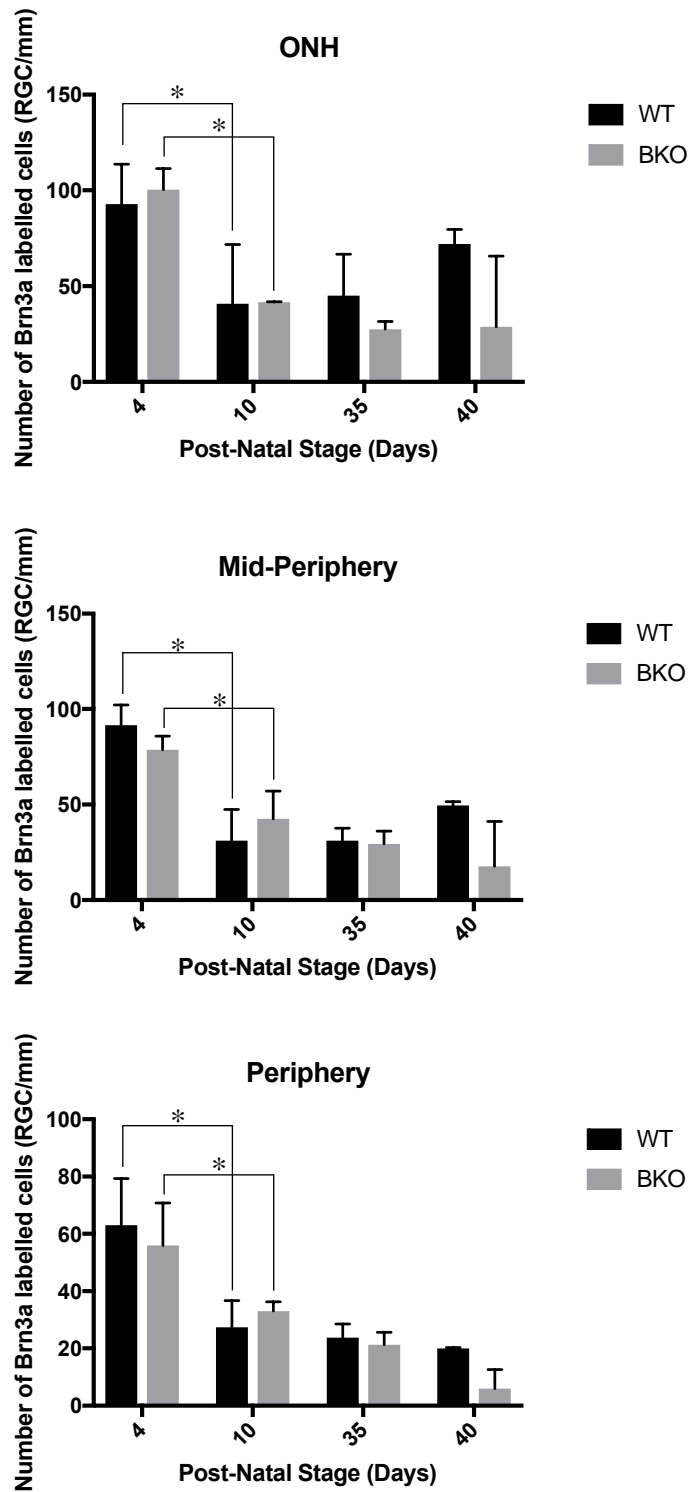


Figure 12: The change in number of *brn3a* labelled cells with respect to time in the wild-type and AP-2β NCC KO. Bar graph denoting the change in *brn3a* labelled cells with respect to time in the wild-type and AP-2β NCC KO. (mean ± 95% CI; * $p < 0.05$, $n = 3$ eyes, 6 measurements)

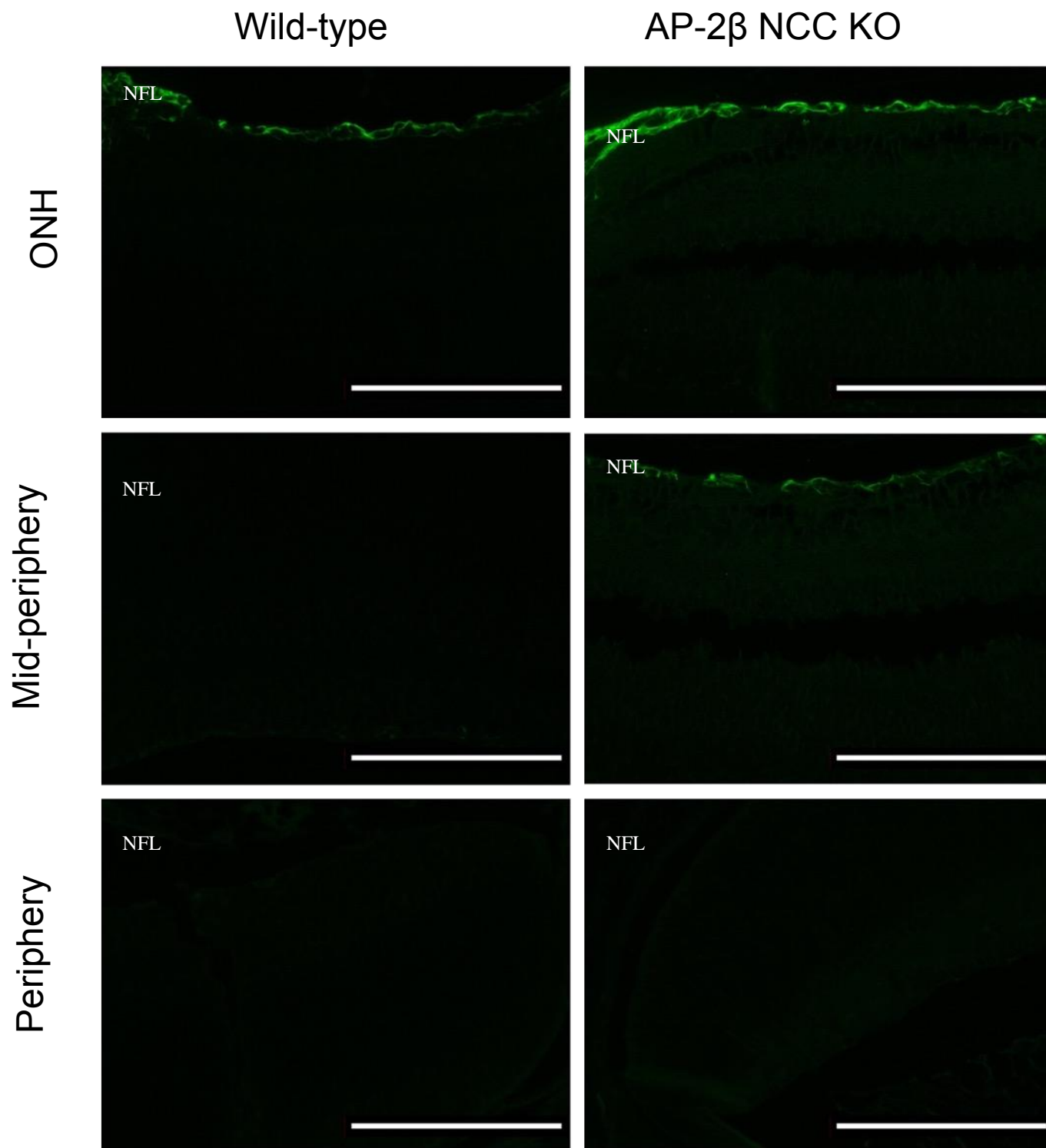


Figure 13: GFAP expression in postnatal day 4 wild-type and AP-2 β NCC KO. Glial Fibrillary Acidic Protein (GFAP) (green) in the wild-type and AP-2 β NCC KO retina. ONH represents the retina adjacent to the Optic nerve, mid-periphery represents the middle of the retina, and the periphery represents the retina adjacent to the ciliary body. Nerve Fiber Layer (NFL). Scale bars: 100 μ m

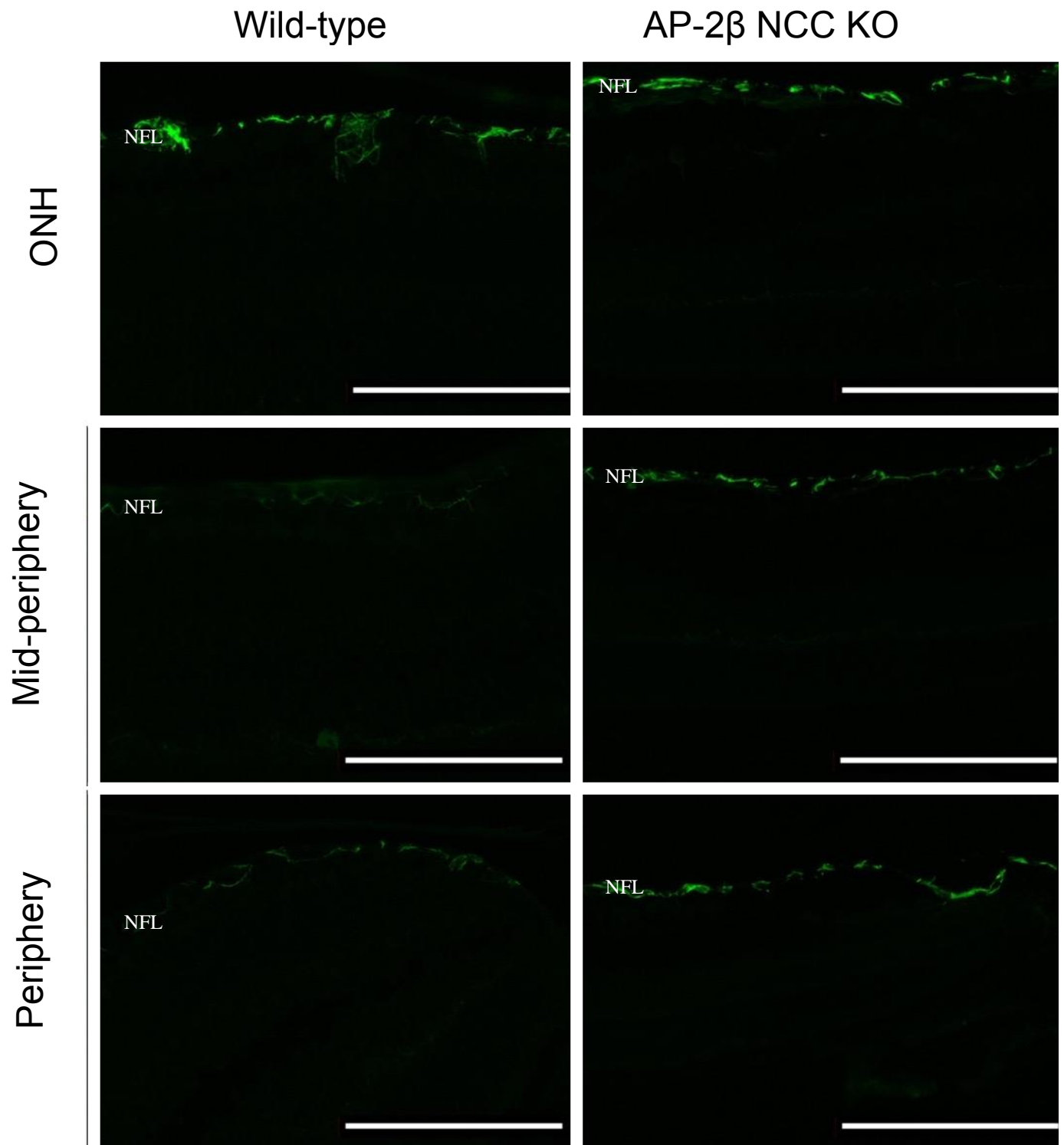


Figure 14: GFAP expression in postnatal day 10 wild-type and AP-2β NCC KO. Glial Fibrillary Acidic Protein (GFAP) (green) in the wild-type and AP-2β NCC KO retina. ONH represents the retina adjacent to the Optic nerve, mid-periphery represents the middle of the retina, and the periphery represents the retina adjacent to the ciliary body. Nerve Fiber Layer (NFL). Scale bars: 100 μ m

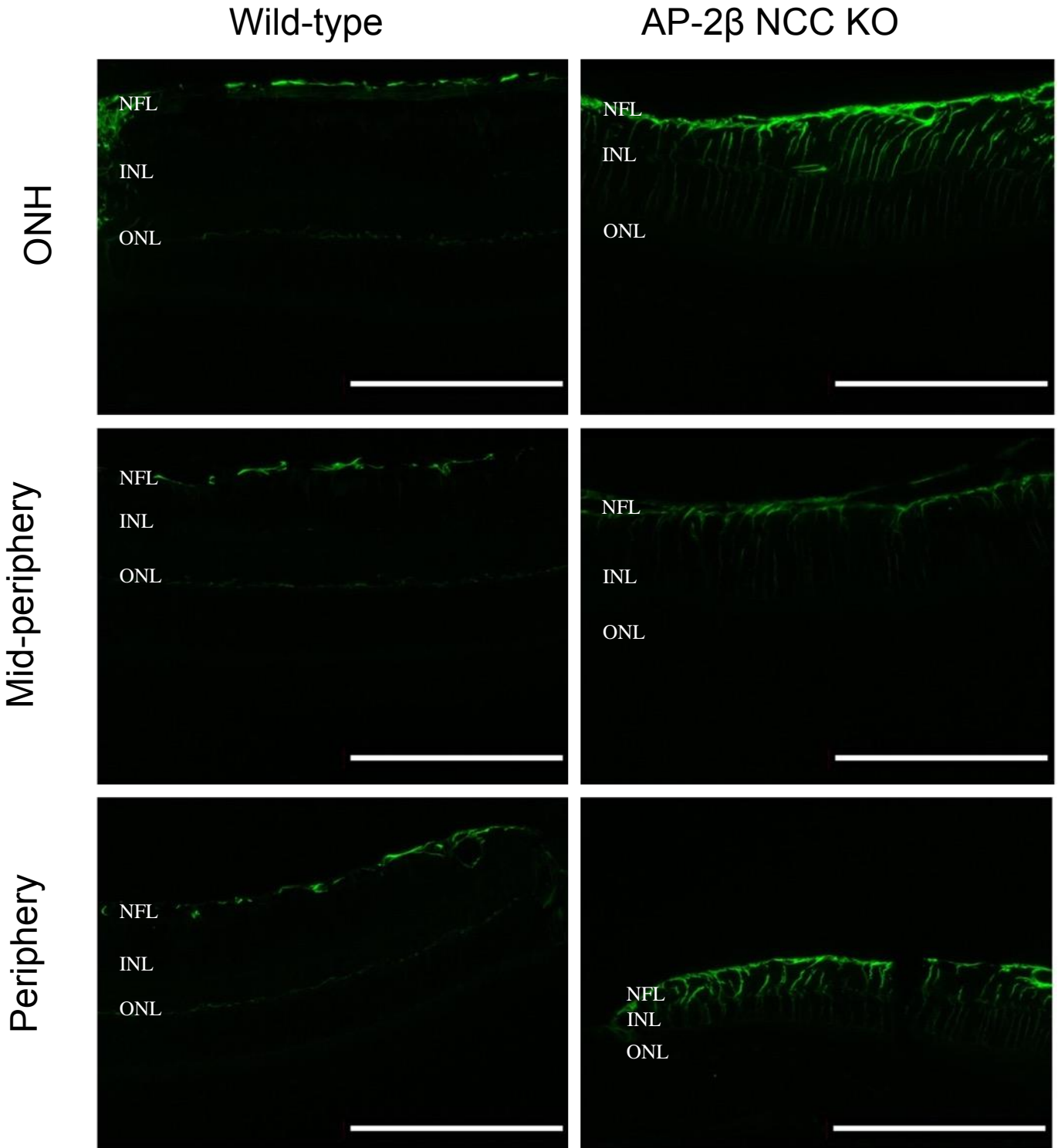


Figure 15: GFAP expression in postnatal day 35 wild-type and AP-2β NCC KO. Glial Fibrillary Acidic Protein (GFAP) (green) in the wild-type and AP-2β NCC KO retina. ONH represents the retina adjacent to the Optic nerve, mid-periphery represents the middle of the retina, and the periphery represents the retina adjacent to the ciliary body. Nerve Fiber Layer (NFL), Inner Nuclear Layer (INL), Outer Nuclear Layer (ONL). Scale bars: 100 μm

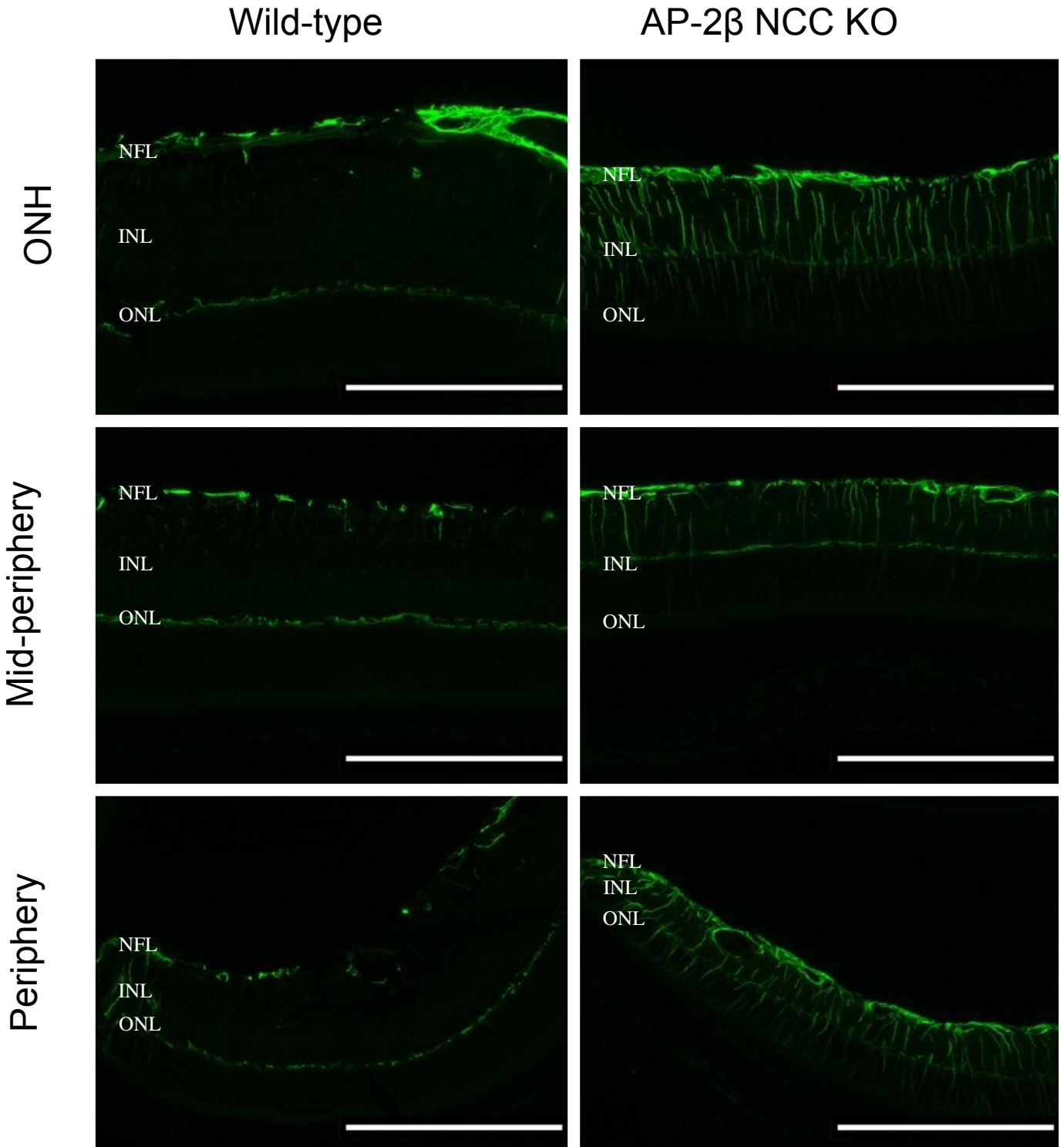


Figure 16: GFAP expression in postnatal day 40 wild-type and AP-2β NCC KO. Glial Fibrillary Acidic Protein (GFAP) (green) in the wild-type and AP-2β NCC KO retina. ONH represents the retina adjacent to the Optic nerve, mid-periphery represents the middle of the retina, and the periphery represents the retina adjacent to the ciliary body. Nerve Fiber Layer (NFL), Inner Nuclear Layer (INL), Outer Nuclear Layer (ONL). Scale bars: 100 μm

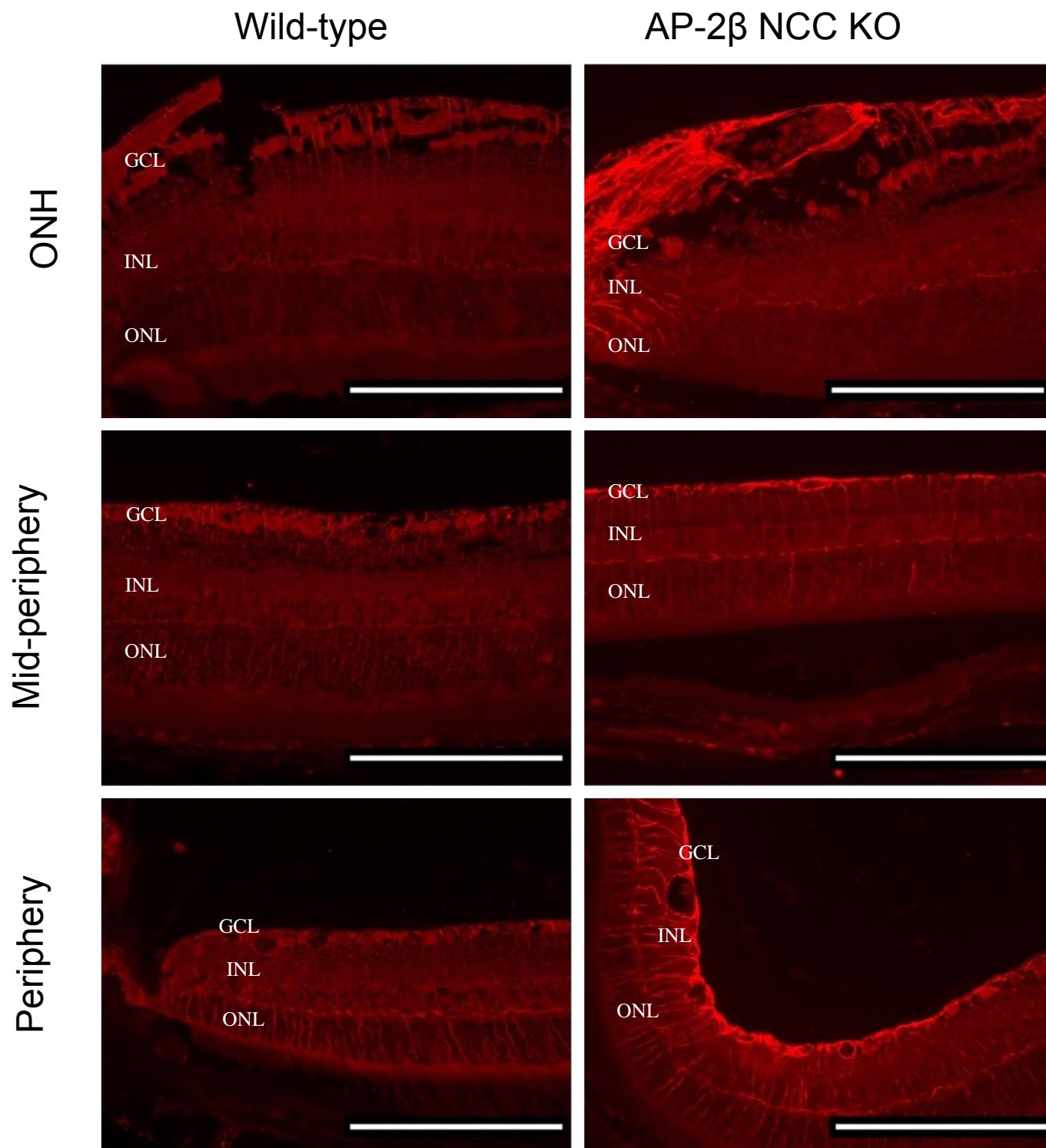


Figure 17: Vimentin expression in postnatal day 40 wild-type and AP-2β NCC KO. Vimentin (red) in the wild-type and AP-2β NCC KO retina. ONH represents the retina adjacent to the Optic nerve, mid-periphery represents the middle of the retina, and the periphery represents the retina adjacent to the ciliary body. Ganglion Cell Layer (GCL), Inner Nuclear Layer (INL), Outer Nuclear Layer (ONL). Scale bars: 100 μ m

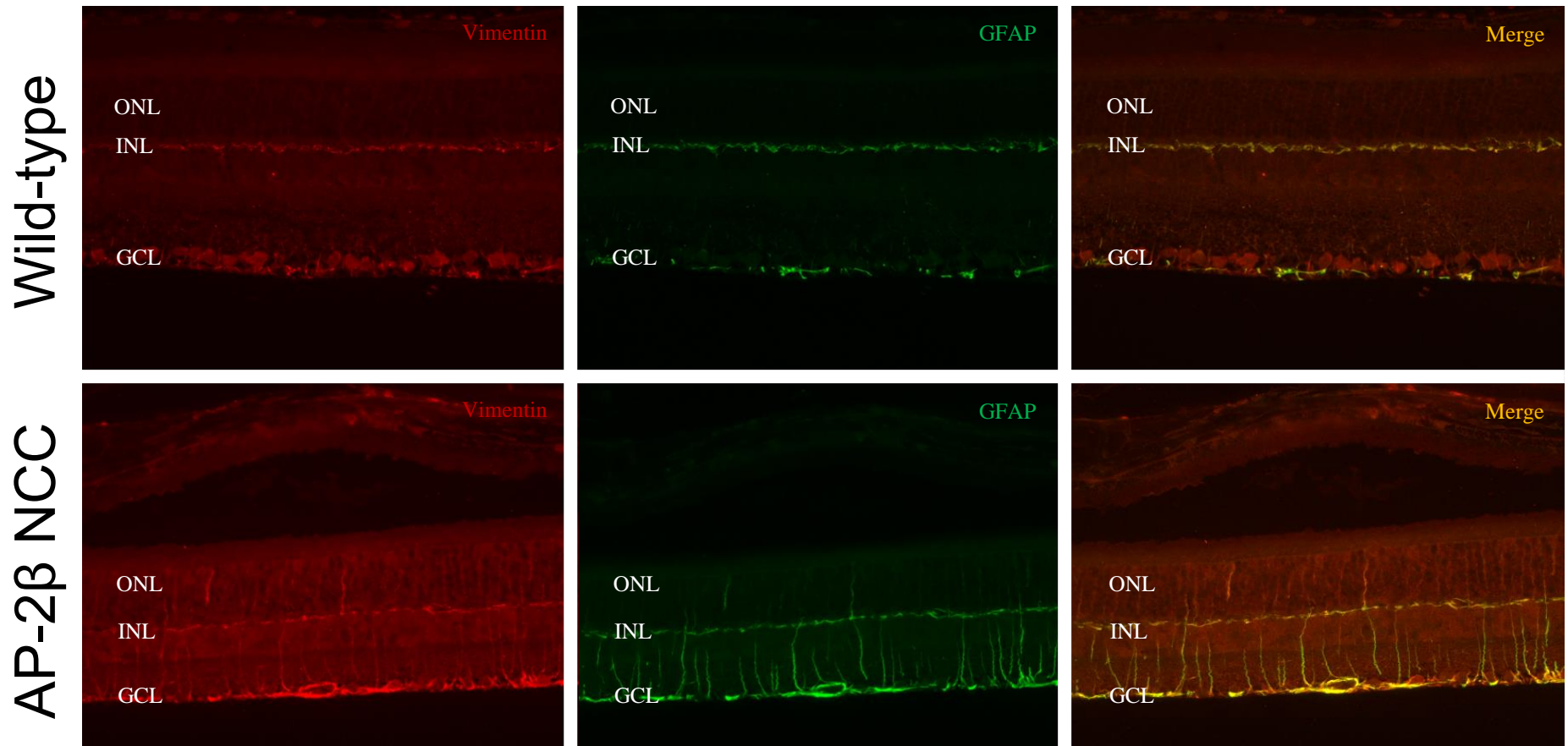


Figure 18: Colocalization of vimentin and GFAP expression in the postnatal day 40 wild-type and AP-2β NCC KO. Glial Fibrillary Acidic Protein (GFAP) (green) and vimentin (red) colocalization (merge) in the wild-type and AP-2β NCC KO midperipheral retina. Ganglion Cell Layer (GCL), Inner Nuclear Layer (INL), Outer Nuclear Layer (ONL). Scale bars: 100 μ m

Tables

Table 1: 1X Master mix recipes: Recipes for *tcfap2β* and *wnt1cre* transgene PCRs

	<i>tcfap2β</i>	<i>wnt1cre</i> transgene
Red Taq Mix (μL)	12.5	12.5
Primer Combo (μL)	0.3	0.4
Water (μL)	7.2	7.1

Table 2: PCR protocol: Table denoting the protocols used for PCR experiments and products.

Alleles	Primers	PCR conditions	Products
<i>wnt1cre</i>	<i>Cre1</i> 5' – GCT GGT TAG CAC CGC AGG TGT AGA G-3'	45 seconds at 95°C 1 minute at 67°C 1 minute and 10 seconds at 72°C	Presence of <i>wnt1cre</i> transgene at 420bp
	<i>Cre3</i> 5' – CGC CAT CTT CCA GCA GGC GCA CC – 3'	(33 cycles)	
<i>tcfap2β</i>	<i>PGK – PolyA DW</i> 5' – CTG CTC TTT ACT GAA GGC TCT TT – 3'	45 seconds at 95°C 45 seconds at 58°C 1 minute at 72°C	Presence of disrupted <i>tcfapβ</i> gene at 380bp
	<i>4 Exon Rev</i> 5' – TTC TGA GGA CGC CGC CCA GG – 3'	(37 cycles)	
	<i>4 Exon DW</i> 5' – CCT CCC AAA TCT GTG ACT TCT – 3'		

Table 3: Antibodies used for immunohistochemistry

Antibody	Host	Manufacturer	Dilution
Anti-Brn3a primary	Goat	Santa Cruz	1:200
Anti-GFAP primary	Rabbit	Dako	1:1000
Anti-Vimentin primary	Goat	Abcam	1:500
Alexa Fluor 488 secondary	Goat or Donkey	Invitrogen – Molecular probes	1:200
Alexa Fluor 568 secondary	Goat or Donkey	Invitrogen – Molecular probes	1:200

Table 4: Summary of ANOVA results for region adjacent to Optic Nerve Head (ONH). Number of brn3a labelled cells at the level of the ONH was analyzed using a 2-way independent ANOVA (* denotes significance). Significant factors were investigated using Tukey multiple comparisons post-hoc test.

Variable	ANOVA F value	Adjusted p value from ANOVA
Interaction	2.352	0.1108
Age	8.721	0.0012 (*)
Phenotype	0.9277	0.3498

Table 5: Summary of ANOVA results for region at middle of retina (mid-periphery). Number of brn3a labelled cells at the level of the mid-periphery was analyzed using a 2-way independent ANOVA (* denotes significance). Significant factors were investigated using Tukey multiple comparisons post-hoc test.

Variable	ANOVA F value	Adjusted p value from ANOVA
Interaction	3.66	0.0351 (*)
Age	26.25	<0.0001 (*)
Phenotype	1.532	0.2337

Table 6: Summary of ANOVA results for region adjacent to ciliary body (periphery). Number of brn3a labelled cells at the level of the periphery was analyzed using a 2-way independent ANOVA (* denotes significance). Significant factors were investigated using Tukey multiple comparisons post-hoc test.

Variable	ANOVA F value	Adjusted p value from ANOVA
Interaction	0.9411	0.4439
Age	29.16	<0.0001 (*)
Phenotype	2.285	0.1502